

Coordinated Defense Allocation in Reach-Avoid Scenarios with Efficient Online Optimization

Junwei Liu, Zikai Ouyang, Jiahui Yang, Hua Chen, Haibo Lu and Wei Zhang

Abstract—Deriving strategies for multiple agents under adversarial scenarios poses a significant challenge in attaining both optimality and efficiency. In this paper, we propose an efficient defense strategy for cooperative defense against a group of attackers in a convex environment. The defenders aim to minimize the total number of attackers that successfully enter the target set without prior knowledge of the attacker’s strategy. Our approach involves a two-scale method that decomposes the problem into coordination against a single attacker and assigning defenders to attackers. We first develop a coordination strategy for multiple defenders against a single attacker, implementing online convex programming. This results in the maximum defense-winning region of initial joint states from which the defender can successfully defend against a single attacker. We then propose an allocation algorithm that significantly reduces computational effort required to solve the induced integer linear programming problem. The allocation guarantees defense performance enhancement as the game progresses. We perform various simulations to verify the efficiency of our algorithm compared to the state-of-the-art approaches, including the one using the Gazabo platform with Robot Operating System.

Index Terms—Multirobot systems, coordination, task allocation, optimization and optimal control.

I. INTRODUCTION

In the domain of multirobot systems, the intricate dynamics arising from robot interactions often necessitate cooperation among team members and competition between distinct teams. Multiplayer adversarial games, characterized by their competitive nature and conflicting objectives, serve as an ideal platform to investigate the delicate interplay between cooperation and competition. Multiplayer adversarial games have been applied to a wide range of real-world applications, including search and rescue [1], autonomous vehicles [2], and security [3]. Nevertheless, attaining optimality and efficiency in solving multiplayer adversarial games remains a formidable challenge due to the high dimensionality of the solution space, the need for rapid decision-making, and the uncertainty introduced by the opposing agents’ strategies. Despite differential games and reinforcement learning offering promising tools, both approaches encounter difficulties when scaling to numerous agents or high-dimensional state spaces, leading to increased

computational complexity when seeking strategies that meet optimal and efficient requirements.

This paper delves into a subclass of multiplayer adversarial games, known as multiplayer reach-avoid games, wherein two teams strive to attack or defend a target set without awareness of their opponent’s strategies. The significance of reach-avoid games lies in their connections to other adversarial games, such as pursuit-evasion [4], [5], capture-the-flag [6], [7], and perimeter defense [8], [9]. In a typical multiplayer reach-avoid game, the attacker team aims to infiltrate the target set with as many robots as possible while avoiding capture, whereas the defender team seeks to prevent these incursions. In this work, we concentrate on the defensive perspective in multiplayer reach-avoid games within convex environments, proposing a robust strategy for the defender team to minimize the number of successful attackers entering the target set, irrespective of the attackers’ decisions. The intricacy of our problem is primarily rooted in the dual requirements of real-time adaptation for optimal response to the dynamic nature of adversaries’ tactics, and maintaining scalability as the number of attacking and defending robots increases.

To overcome these challenges, we propose a two-scale strategy for the defender team by dividing the problem into two subproblems: 1) coordinating a group of defenders against a single attacker; and 2) allocating defenders to the attackers present in the game. The defense coordination concerning a single attacker primarily determines the binary outcome of whether a group of defenders can successfully protect the target set, or in other words, win against the attacker. Based on the results of all potential binary outcomes between defenders and a single attacker, the defense allocation aims to optimally assign defenders to attackers with the goal of minimizing the number of successful attackers entering the target set. In particular, we develop online optimization techniques for both subproblems, ensuring our approach’s real-time adaptability and scalability in the context of dynamic interactions.

As the foundation of our framework, we present a dual-mode switching algorithm to coordinate a group of defenders against a single attacker. Our approach continuously switches between two distinct defense strategies that dynamically adapt to the joint state of the defender group and the attacker. Particularly, one of these strategies corresponds to a defense-winning region of initial joint states, ensuring victory for the defenders against any admissible attack strategy. Moreover, each defense strategy is implemented through the online resolution of a convex program. The underlying principle behind our approach hinges on leveraging the concept of the safe-reachable set to devise two separate objective functions. The safe-reachable set represents the collection of positions an attacker can reach without being captured by any defender, given the current

Junwei Liu and Hua Chen are with the School of System Design and Intelligent Manufacturing, Southern University of Science and Technology, Shenzhen 518055, China {liujw, chenh6}@sustech.edu.cn

Zikai Ouyang and Wei Zhang are with the School of System Design and Intelligent Manufacturing, Southern University of Science and Technology, Shenzhen 518055, China, and also with the Peng Cheng Laboratory, Shenzhen 518000, China ouyang2022@mail.sustech.edu.cn, zhangw3@sustech.edu.cn

Jiahui Yang is with the Department of Mechanical and Energy Engineering, Southern University of Science and Technology, Shenzhen 518055, China 11911213@mail.sustech.edu.cn

Haibo Lu is with the Peng Cheng Laboratory, Shenzhen 518000, China luhb@pcl.ac.cn

joint state. By integrating these objective functions, the defense coordination problem can be effectively transformed into an online robust maximization problem, where the robustness accounts for the worst-case scenario the attacker could employ. Solving this online robust maximization problem subsequently yields the corresponding defense strategy. Our proposed algorithm ensures the maximization of the defense-winning region while maintaining real-time operational capabilities, providing a robust and efficient solution for defense coordination in single-attacker scenarios.

Building upon the defense coordination results introduced earlier, we further develop a monotonic defense enhancement algorithm designed to optimally allocate defenders to attackers engaged in the game. Our approach employs a heuristic method to tackle an integer linear program (ILP) while incorporating a monotonicity constraint. This constraint guarantees that the expected number of attackers unable to reach the target set is monotonically non-decreasing over time, leading to a sustained improvement in defense performance as the game progresses. At the core of our algorithm is a hierarchical iterative technique that approximates the solution to the ILP problem, which is formulated using an objective function based on the safe-reachable sets of all attackers. By incorporating the concepts of active defense set and irreducibility, we establish hierarchical levels that facilitate the derivation of a suboptimal solution. Our proposed algorithm offers a computationally efficient and effective defense allocation solution for multi-attack scenarios in multiplayer reach-avoid games, significantly reducing the number of game outcomes required to determine the objective function within the ILP problem.

A. Related Work

The traditional approach for multi-player reach-avoid games relies on the framework of addressing differential games [10], [11]. The core of this approach is to solve the Hamilton-Jacobi-Isaacs (HJI) equation or its variant offline, and subsequently utilize the stored data to generate the barrier and optimal strategies [12]. The barrier is defined by the two maximum winning regions, one of which consists of all points where the joint state initializes can ensure a victory regardless of the opponent's strategies. The limitation of the HJI method as well as its numerical approximation lies in the induced computational burden [11], [13], which heavily restricts the number of players.

On the other hand, multi-player reach-avoid games can be solved based on some geometric features. In [14], a two-player reach-avoid game was first studied and the optimal strategies were found in terms of the perpendicular bisector between defender and attacker. The work of [15] derived the closed-form barrier and associated optimal strategies for a two-defender single-attacker scenario in a 3-D space with point capture, and the method was further applied to more general multi-player systems in a 2-D space with a linear target [16]. The two-defender single-attacker reach-avoid game was also considered in [17], where the target set is constrained to a line segment. This work provided an exact construction of the

barrier by means of the Apollonius circle, and the idea was further extended to handle multiplayer systems in more general 2-D convex domains [18].

The idea of SRS dates back to the pioneering work of Isaacs on the differential game [14], where the explicit form of the SRS was given for a two-player reach-avoid game without formal proof. Zhou et al. [19] later introduced the SRS concept to a multiplayer pursuit-evasion game within a general environment, whereas no explicit form was given.

B. Contributions

Our main contributions are as follows:

- 1) Our algorithm is applicable to an extensive range of convex environments in n -dimensional space with a nonzero capture radius, extending beyond the existing results in [18], [20], which only consider simpler conditions.
- 2) Our single-attack defense coordination result identifies the maximum defense-winning region for defenders, enhancing the current state-of-the-art as presented in [15], [21].
- 3) Our multiple-attack defense allocation result ensures a continuous improvement in performance as time progresses. To the best of our knowledge, this is a novel contribution not yet found in the existing literature.
- 4) Our algorithm strikes a balance between optimality and efficiency, as demonstrated through real-world scenario simulations, making it a valuable solution for practical robotic defense systems.

C. Organization and Notation

The remainder of the paper is organized as follows. In section II, we formulate our problem as a minimax optimal control problem, which is then decomposed as single-attack defense coordination problem and multi-attack defense allocation problem. In Section III, we develop an algorithm against a single attacker. Then in Section IV, we present an algorithm for defense allocation. We demonstrate our result in Section V, and show that ours outperform some of the existing results.

The notation used throughout this paper is summarized as follows. Let \mathbb{R}^n be the n -dimensional Euclidean space and $\|\cdot\|$ be the Euclidean norm. Let $\mathbb{R}_{\geq 0}$ denote the set of nonnegative real numbers. Let $\mathcal{N}(v)$ be the normalizer to a vector v : $\mathcal{N}(v) = \frac{v}{\|v\|}$ if $v \neq 0$ and 0 otherwise. In the scalar case, \mathcal{N} is nothing but the sign function. Given a set S , let $\mathbf{1}_S(\cdot)$ denote the indicator function of S , i.e., $\mathbf{1}_S(x) = 1$ if $x \in S$ and 0 otherwise, and let $|S|$ be the cardinal number of S . Given a set of vectors v_1, \dots, v_n , we use (v_1, \dots, v_n) to denote the column vector consisting of the entries of v_i for $i = 1, \dots, n$ in sequence. \mathcal{D}^{N+M} denotes the Cartesian product of $N+M$ copies of the domain \mathcal{D} .

II. PROBLEM FORMULATION

Consider a multiplayer reach-avoid game involving a team of defender robots (called *defenders*) competing against a team of attacker robots (called *attackers*) within a confined *domain* containing a designated *target set*. The primary objective of the attacker team is to deploy as many robots as possible to

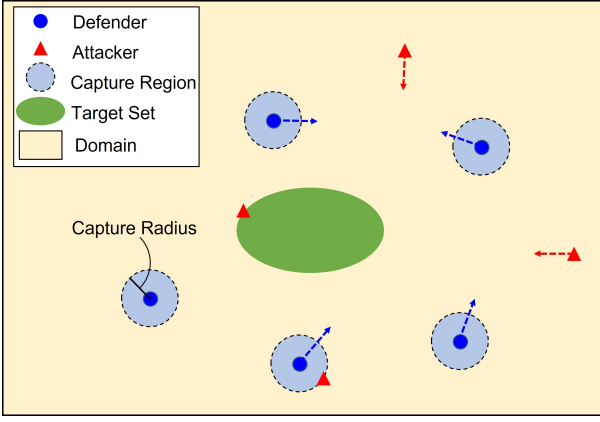


Fig. 1. A 2D instance of a multiplayer reach-avoid game.

reach the target set while avoiding capture by any defender, whereas the defender team strives to prevent the attackers from entering the target set. An illustrative depiction of this game is provided in Fig. 1. This paper primarily focuses on the defense perspective, wherein we aim to develop a strategy for the defending team to minimize the total number of attackers that successfully reach the target set, without prior knowledge of the attackers' strategy.

We study scenarios where the domain and target set, denoted as \mathcal{D} and \mathcal{G} respectively, are bounded, closed, and convex. Concretely, we assume that \mathcal{D} and \mathcal{G} are defined by the zero sublevel sets of smooth convex functions d_k and g_l , with $k \in \mathcal{I}_D$ and $l \in \mathcal{I}_G$, as follows:

$$\mathcal{D} = \{q \in \mathbb{R}^n \mid \max_{k \in \mathcal{I}_D} d_k(q) \leq 0\} \quad (1)$$

$$\mathcal{G} = \{q \in \mathbb{R}^n \mid \max_{l \in \mathcal{I}_G} g_l(q) \leq 0\}. \quad (2)$$

In this context, we model the robots as particles, with defenders indexed by $\mathcal{N} = \{1, \dots, N\}$ and attackers indexed by $\mathcal{M} = \{1, \dots, M\}$. Besides, the robots are assumed to move within the domain \mathcal{D} with single-integrator dynamics:

$$\dot{p}_i^d = u_i^d, \quad \forall i \in \mathcal{N} \quad (3)$$

$$\dot{p}_j^a = u_j^a, \quad \forall j \in \mathcal{M} \quad (4)$$

where p_i^d and u_i^d (resp. p_j^a and u_j^a) represent the position and velocity of defender i (resp. attacker j).

We define $x = (p_1^d, \dots, p_N^d, p_1^a, \dots, p_M^a)$ as the *joint state* of the system (3)-(4). Thus, the joint state satisfies the constraint:

$$x \in \mathcal{D}^{N+M}. \quad (5)$$

Additionally, we define the *control inputs* of defender i and attacker j as u_i^d and u_j^a , respectively. These control inputs are subject to the following constraints:

$$u_i^d \in \mathcal{U}_i^d = \{v_i^d \in \mathbb{R}^n \mid \|v_i^d\| \leq v_{i,\max}^d\}, \quad \forall i \in \mathcal{N} \quad (6)$$

$$u_j^a \in \mathcal{U}_j^a = \{v_j^a \in \mathbb{R}^n \mid \|v_j^a\| \leq v_{j,\max}^a\}, \quad \forall j \in \mathcal{M}. \quad (7)$$

Here, $v_{i,\max}^d$ and $v_{j,\max}^a$ are the maximum speeds of defender i and attacker j , respectively. To prevent attackers from easily outrunning defenders, we impose a constraint on the maximum

speed ratio, requiring that defenders possess equal or greater speed capabilities than attackers:

$$\gamma_{ij} = \frac{v_{i,\max}^d}{v_{j,\max}^a} \geq 1, \quad \forall (i, j) \in \mathcal{N} \times \mathcal{M} \quad (8)$$

where γ_{ij} denotes the ratio of defender i 's maximum speed relative to that of attacker j .

In the multiplayer reach-avoid game, interactions between defenders and attackers are determined by their relative positions. Specifically, attacker j is said to be *captured* by defender i if the distance between their positions is less than a positive constant r_i :

$$\|p_j^a - p_i^d\| < r_i \quad (9)$$

where r_i represents the i th *capture radius*. This leads to the *capture region* of defender i defined as $\mathcal{R}_i = \{q \in \mathcal{D} \mid \|q - p_i^d\| < r_i\}$. To simplify our analysis, we assume that attackers that have been captured or have reached the target set become stationary, while defenders can proceed with their tasks after capturing an attacker. This assumption allows us to focus on those attackers that have not been captured or have not yet reached the target set, indexed by $\mathcal{M}_a = \{j \in \mathcal{M} \mid \rho_j(x_j) = 1\}$, where $x_j = (p_1^d, \dots, p_N^d, p_j^a)$ and ρ_j is defined as:

$$\rho_j(x_j) = \begin{cases} 0, & p_j^a \in \mathcal{G} \text{ or } \min_{i \in \mathcal{N}} (\|p_j^a - p_i^d\| - r_i) < 0 \\ 1, & \text{otherwise.} \end{cases} \quad (10)$$

Keeping this in mind, we can modify the input constraint for attacker j as follows:

$$u_j^a \in \tilde{\mathcal{U}}_j^a(x_j) = \rho_j(x_j) \mathcal{U}_j^a, \quad \forall j \in \mathcal{M}. \quad (11)$$

In this game, we adopt a state feedback information pattern wherein each team makes decisions according to the current joint state without accessing the control inputs of the opposing team. Under this information pattern, an *admissible* strategy for defender i (resp. attacker j) is defined as a mapping from the joint state x to the input constraint set \mathcal{U}_i^d (resp. $\tilde{\mathcal{U}}_j^a(x_j)$) such that $u_i^d = \pi_i^d(x)$ (resp. $u_j^a = \pi_j^a(x)$). We define an admissible defense strategy as the collection of all defenders' admissible strategies, denoted by $\pi^d = (\pi_1^d, \dots, \pi_N^d)$. Likewise, an admissible attack strategy, denoted by $\pi^a = (\pi_1^a, \dots, \pi_M^a)$, is defined as the collection of all attackers' admissible strategies.

The outcome of the multiplayer reach-avoid game is evaluated in terms of a payoff function, which quantifies the total number of attackers reaching the target set up to the terminal time t_f . We consider the terminal time t_f to be free, indicating that the game continues until there are no active attackers left. Given an initial joint state x_0 and a pair of admissible defense and attack strategies π^d and π^a , the payoff function is formally defined as:

$$J(x_0, \pi^d, \pi^a) = \sum_{j \in \mathcal{M}} \mathbf{1}_{\mathcal{G}}(p_j^a(t_f)). \quad (12)$$

It is important to note that in some cases, the game may not terminate if at least one active attacker cannot be eliminated. The goal of the defender team is to minimize the value of the payoff function J by choosing appropriate defense strategies, regardless of any admissible attack strategy.

Problem 1 (Cooperative Defense in Multiplayer Reach-Avoid Games): Given a domain \mathcal{D} and a target set \mathcal{G} as defined by (1) and (2), along with an initial joint state x_0 of the system (3)-(4), we seek to find an admissible defense strategy π^d that minimizes the payoff function J against any admissible attack strategy π^a . This corresponds to solving the following minimax optimal control problem:

$$\begin{aligned} & \min_{\pi^d} \max_{\pi^a} J(x_0, \pi^d, \pi^a) \\ & \text{s.t. } x(0) = x_0, \text{ (3), (4), (5), (6), (8), (11).} \end{aligned}$$

Solving Problem 1 poses significant challenges due to several factors, such as the high dimensionality of the joint state, the discreteness of the payoff function, and the presence of both cooperative and competitive interactions among agents. A widely used approach to tackling these challenges is to employ the differential game formulation, which involves solving the HJI equation or its invariant. However, as the dimension of the joint state increases, the computational complexity of this method becomes intractable, particularly in multi-agent scenarios.

To tackle the aforementioned challenges, we decompose Problem 1 into two interconnected subproblems:

- **Single-Attack Defense Coordination Problem:** Given a coalition of defenders and a single attacker, design an admissible strategy for the coalition to prevent the attacker from reaching the target set, irrespective of any admissible strategy employed by the attacker. In this context, a *coalition* refers to a group of defenders collaboratively working to protect against a specific attacker.
- **Multi-Attack Defense Allocation Problem:** Building upon the solution to the Single-Attack Defense Coordination Problem, design an allocation algorithm that assigns coalitions to active attackers, with the objective of minimizing the payoff function. In this context, active attackers are defined as those that have neither been captured nor successfully reached the target set.

The Single-Attack Defense Coordination Problem is solved in a continuous-time manner, wherein the outcome of the multiplayer reach-avoid game is binary: the attacker either succeeds in reaching the target set or is captured outside the target set. We say that the coalition *wins* if the attacker can never enter the target set; otherwise, the coalition is considered *defeated*. Consequently, the problem of single-attack defense coordination is to find a winning strategy for the coalition against the attacker. Conversely, the Multi-Attack Defense Allocation Problem is handled in a discrete-time framework, where each time instant corresponds to an implementation of the allocation. We refer to these time instants as *allocation times*. At each allocation time, the allocation algorithm reevaluates the assignment of active attackers to coalitions based on the current joint state.

Integrating the solutions of these two subproblems results in a holistic solution to Problem 1. Given the current joint state, we initially identify the set of active attackers \mathcal{M}_a by checking their relative distances to the defenders up to the last time instant. Subsequently, the solution to the Multi-Attack Defense Allocation Problem dictates the assignment of active

attackers to coalitions. For each specified coalition-attacker pair, we then apply the solution to the Single-Attack Defense Coordination Problem to compute the control input for each defender in the corresponding coalition. This two-scale scheme continues to update in real-time, effectively decomposing the high-dimensional, complex minimax optimal control problem into smaller, more tractable problems.

III. DEFENSE COORDINATION AGAINST A SINGLE ATTACKER

In this section, we present a defense strategy for a coalition in multiplayer reach-avoid games involving a single attacker. Our approach begins with a formal definition of the safe-reachable set and a derivation of its sublevel set representation. Leveraging the minimum squared distance between the safe-reachable set and the target set, we construct an objective function that transcribes the single-attack defense coordination problem into its online robust maximization. The solution to this robust maximization leads to an online convex programming-based defense strategy, which guarantees the coalition's victory for a specific region of initial joint states. To increase the chances of winning against non-optimal attack strategies, we further propose a dual-mode switching defense strategy to fit with all initial joint states.

A. Safe-Reachable Set

In the case of a single attacker, the multiplayer reach-avoid game is reduced to a Hamilton-Jacobi reachability problem, in which the binary outcome of an initial joint state is determined by the reach-avoid set [10]. This set comprises joint states from which the attacker can reach the target set without being captured by any of the defenders. By solving an HJI equation numerically, the reach-avoid set can be represented as a sublevel set of the HJI solution [22]. However, the backward computation associated with this method suffers from the curse of dimensionality, hindering its application to multi-agent systems [13]. In contrast, the safe-reachable set seeks to collect the attacker's reachable locations that remain capture-free given the current joint state [19]. This set can be computed using forward computation, which only concerns the attacker's position state and does not involve solving for the target set reachability, making it more computationally efficient. We will demonstrate that under our problem settings, the binary outcome of an initial joint state can also be characterized by the safe-reachable set.

A formal definition of the safe-reachable set for a coalition-attacker pair is given below. Consider a coalition \mathcal{C} and an attacker j with dynamics described by (3) and (4), respectively, and denote their joint state as $x_j^{\mathcal{C}} = (p_i^d, i \in \mathcal{C}; p_j^a)$. In light of (9), the capture-free condition for attacker j can be expressed as follows:

$$\max_{i \in \mathcal{C}} s_i(p_i^d, p_j^a) \leq 0 \quad (13)$$

where $s_i(p_i^d, p_j^a) = r_i - \|p_i^d - p_j^a\|$. To account for the dependence of agent trajectories on their initial states and strategies, we introduce the notations $\chi_j^a(\cdot; p_j^a(0), \pi_j^a)$ and $\chi_i^d(\cdot; p_i^d(0), \pi_i^d)$, which respectively denote the trajectory of

attacker j over time starting from $p_j^a(0)$ using the attack strategy π_j^a , and the trajectory of defender i over time starting from $p_i^d(0)$ using the defense strategy π_i^d .

Definition 1 (Safe-Reachable Set): Given a joint state x_j^c of (\mathcal{C}, j) , the *safe-reachable set* (SRS) $\Omega_j^c(x_j^c)$ for attacker j induced by the coalition \mathcal{C} consists of all positions $q \in \mathcal{D}$ satisfying the following properties:

- 1) (Reachability) There exists a time instant τ and an admissible attack strategy π_j^a over the interval $[0, \tau]$ such that the attacker j can reach position q at time τ :

$$q = \chi_j^a(\tau; p_j^a, \pi_j^a);$$

- 2) (Safety) For any admissible defense strategy π_i^d used by the defenders $i \in \mathcal{C}$, the capture-free condition (13) holds for all $t \in [0, \tau]$:

$$\max_{i \in \mathcal{C}} s_i(\chi_i^d(t; p_i^d, \pi_i^d), \chi_j^a(t; p_j^a, \pi_j^a)) \leq 0, \quad \forall t \in [0, \tau].$$

The SRS offers a predictive way to evaluate the capture-free condition (13) by incorporating the dynamic and input constraints of both opponents. When the SRS is nonempty, it implies that the attacker is currently situated within the SRS, and the capture-free condition is satisfied for the current joint state, as per Definition 1. Moreover, the size of the SRS can be used to anticipate the attacker's ability to move freely without compromising safety. A larger SRS indicates that the attacker has more options for safe movement, regardless of any defense strategies that may be employed.

Similar to the reach-avoid set, the SRS admits a sublevel set representation. Consider a point q inside the SRS that attacker j can reach at time τ . Simultaneously, defender i can arrive at point $q_i^d = p_i^d + v_{i, \max}^d \frac{q - p_i^d}{\|q - p_i^d\|} \tau$ using the constant strategy $v_{i, \max}^d \frac{q - p_i^d}{\|q - p_i^d\|}$. According to Definition 1, q adheres to the capture-free condition $\max_{i \in \mathcal{C}} s_i(q_i^d, q) = \max_{i \in \mathcal{C}} (r_i - \|q - p_i^d\| - v_{i, \max}^d \tau) \leq 0$. On the other hand, since attacker j can safely reach q , the time τ must fulfill $\tau \in [\tau_{\min}, \frac{\|q - p_j^a\|}{v_{j, \max}^a}]$,

with $\tau_{\min} = \frac{\|q - p_j^a\|}{v_{j, \max}^a}$ representing the minimum time for attacker j to reach q . This leads to $\max_{i \in \mathcal{C}} (r_i - \|q - p_i^d\| - v_{i, \max}^d \tau_{\min}) = \max_{i \in \mathcal{C}} (r_i + \gamma_{ij} \|q - p_j^a\| - \|q - p_i^d\|) \leq 0$, which can be rewritten as $\max_{i \in \mathcal{C}} c_{ij}(q, x_{ij}) \leq 0$ with

$$c_{ij}(q, x_{ij}) = (\gamma_{ij} \|q - p_j^a\| + r_i)^2 - \|q - p_i^d\|^2 \quad (14)$$

and $x_{ij} = (p_i^d, p_j^a)$. Moreover, satisfying inequality (14) for every $i \in \mathcal{C}$ is sufficient to ensure that q lies within the SRS.

Proposition 1 (Sublevel Set Representation): The SRS defined in Definition 1 is closed and convex, taking the form

$$\Omega_j^c(x_j^c) = \bigcap_{i \in \mathcal{C}} \left\{ q \in \mathcal{D} \mid c_{ij}(q, x_{ij}) \leq 0 \right\} \quad (15)$$

where c_{ij} is given by equation (14).

Proof: We have shown that $\max_{i \in \mathcal{C}} c_{ij}(q, x_{ij}) \leq 0$ for each $q \in \Omega_j^c(x_j^c)$, and the remaining is detailed in Appendix A. ■

The SRS serves as a generalization of both the Voronoi diagram and Apollonius diagram by accommodating nonzero capture radii. As evident from equation (15), when the capture radii equal zero, the SRS simplifies to the Voronoi cell if

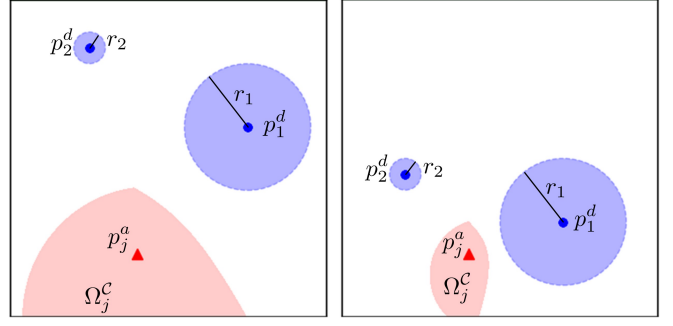


Fig. 2. Visualization of the SRS under different joint states in a 2D domain. The blue disks represent the defenders' capture regions, and the red region illustrates the SRS for a specific attacker. The parameters are chosen as $\gamma_{1j} = 1$, $\gamma_{2j} = 2$, $r_1 = 2$ and $r_2 = 0.5$. As displayed from left to right, the SRS varies with joint states, and its size decreases as the distances between the attacker and the defenders diminish while accounting for the capture radii of the defenders.

$\gamma_{ij} = 1$ and to the Apollonius circle/sphere if $\gamma_{ij} > 1$. Unlike the Voronoi diagram and Apollonius diagram, the SRS partitions the space based on the attacker's capacity to move freely without being captured, factoring in the defenders' capture radii, as depicted in Fig. 2. This distinctive characteristic of the SRS enables a more realistic representation of the interaction between the attacker and defenders, enhancing defense coordination with unpredictable attacker movements.

B. Single-Attack Objective Function

Having the SRS concept, we next develop an objective function for the single-attack defense coordination problem. Given that the SRS pertains to the attacker's forward reachability, it is natural to define an objective function that connects the SRS and the target set in terms of their minimum distance. With this in mind, we propose the minimum squared distance between the SRS and the target set as the objective function, which we refer to as the *single-attack objective function*:

$$\Phi_j^c(x_j^c) = \min_{\substack{q \in \Omega_j^c(x_j^c) \\ \tilde{q} \in \mathcal{G}}} \|q - \tilde{q}\|^2. \quad (16)$$

Since both the SRS and the target set are convex and admit sublevel set representations, according to Proposition 1 and the assumption on the target set, the value of Φ_j^c can be determined by solving the following parametric convex program:

$$\begin{aligned} \min_{(q, \tilde{q}) \in \mathbb{R}^{2n}} \quad & \|q - \tilde{q}\|^2 \\ \text{s.t.} \quad & c_{ij}(q, x_{ij}) \leq 0, \quad \forall i \in \mathcal{C} \\ & d_k(q) \leq 0, \quad \forall k \in \mathcal{I}_D \\ & g_l(\tilde{q}) \leq 0, \quad \forall l \in \mathcal{I}_G \end{aligned} \quad (17)$$

where the joint state x_j^c serves as the parametric vector.

The single-attack objective function provides a quantitative measure for the binary outcome of the single-attacker multi-defender reach-avoid game. It is essential to note that the value of Φ_j^c is always nonnegative for a nonempty SRS, and positive if the intersection between the SRS and the target set is empty. This suggests that retaining the positivity of Φ_j^c is critical in preventing the attacker from reaching the target set.

Consequently, a winning guarantee condition for the coalition can be derived in terms of the single-attack objective function.

Lemma 1 (Defense-Winning Condition): For a given coalition-attacker pair (\mathcal{C}, j) at the initial joint state, the coalition \mathcal{C} is guaranteed to win against attacker j if and only if there exists an admissible defense strategy such that, for any admissible attack strategy, the single-attack objective function remains positive throughout the duration:

$$\Phi_j^{\mathcal{C}}(x_j^{\mathcal{C}}(t)) > 0, \forall t \in [0, t_f).$$

Proof: For sufficiency, if $\Phi_j^{\mathcal{C}}(x_j^{\mathcal{C}}(t))$ remains positive for all $t \in [0, t_f)$, then the SRS cannot intersect the target set during this time interval. Since the attacker's position is always contained within the non-empty SRS, the attacker can never enter the target set. This implies that the coalition is guaranteed to win the game. For necessity, assume for the sake of contradiction that the coalition wins while $\Phi_j^{\mathcal{C}}(x_j^{\mathcal{C}}(T)) = 0$ for some $T \in [0, t_f)$. According to Definition 1, there is an admissible attack strategy starting from time T that drives attacker j to the target set within a finite time. This, however, contradicts the assumption that the coalition wins. ■

Remark 1 (Online Robust Maximization): Lemma 1 confirms that if the strict zero superlevel set of $\Phi_j^{\mathcal{C}}$ is *robustly positively invariant* [23] under an admissible defense strategy, then the coalition can guarantee victory against any admissible attack strategy. The notion of robustness means that the coalition must maximize the single-attack objective function $\Phi_j^{\mathcal{C}}$ for the worst-case attack strategy. As a consequence, the optimal defense coordination problem can be converted into an online robust maximization of the single-attack objective function for the coalition at each joint state.

C. Defense-Winning Strategy

We proceed to derive a defense-winning strategy for the coalition \mathcal{C} by performing online robust maximization of the single-attack objective function $\Phi_j^{\mathcal{C}}$ when it has a positive value. In light of Pontryagin's Maximum Principle for differential games (cf. Theorem 8.2 in [24]), robustly maximizing $\Phi_j^{\mathcal{C}}$ for the coalition \mathcal{C} amounts to robustly maximizing its time derivative $\dot{\Phi}_j^{\mathcal{C}}$ with respect to the inputs $u_i^d, i \in \mathcal{C}$. Note that, the time derivative of $\Phi_j^{\mathcal{C}}$ along the joint state trajectory is given by

$$\dot{\Phi}_j^{\mathcal{C}} = \sum_{i \in \mathcal{C}} \frac{\partial \Phi_j^{\mathcal{C}}}{\partial p_i^d} u_i^d + \frac{\partial \Phi_j^{\mathcal{C}}}{\partial p_j^a} u_j^a. \quad (18)$$

To measure the effect of each agent's input on $\dot{\Phi}_j^{\mathcal{C}}$, we need to determine the gradients of $\Phi_j^{\mathcal{C}}$ concerning the positions of all agents. Fortunately, by invoking the Karush–Kuhn–Tucker (KKT) conditions (cf. Theorem 12.1 in [24]), a linear correspondence can be made almost everywhere between the gradients of $\Phi_j^{\mathcal{C}}$ and those of $c_{ij}, i \in \mathcal{C}$ given in (14).

Proposition 2 (Gradient Correspondence): Suppose the convex program (17) admits a unique solution for each joint

state $x_j^{\mathcal{C}}$ within a region $\mathcal{D}' \subset \mathcal{D}$. Then for almost every $x_j^{\mathcal{C}} \in \mathcal{D}'$, there exist nonnegative constants $\lambda_{ij}^*, i \in \mathcal{C}$ such that

$$\begin{aligned} \frac{\partial \Phi_j^{\mathcal{C}}}{\partial p_i^d} &= \lambda_{ij}^* \frac{\partial c_{ij}}{\partial p_i^d}(\xi_j^{\mathcal{C}}, x_{ij}), \quad \forall i \in \mathcal{C} \\ \frac{\partial \Phi_j^{\mathcal{C}}}{\partial p_j^a} &= \sum_{i \in \mathcal{C}} \lambda_{ij}^* \frac{\partial c_{ij}}{\partial p_j^a}(\xi_j^{\mathcal{C}}, x_{ij}) \end{aligned} \quad (19)$$

where $\xi_j^{\mathcal{C}}$ is the first n -dimensional component of the unique solution to the convex program (17).

Proof: See Appendix B. ■

Proposition 2 provides a tractable procedure for generating a defense strategy that approximately robustly maximizes $\Phi_j^{\mathcal{C}}$, assuming that (20) holds almost everywhere. This procedure entails deriving the gradient of the functions $c_{ij}, i \in \mathcal{C}$ for each $q \in \Omega_j^{\mathcal{C}}(x_j^{\mathcal{C}})$ and $q \neq p_j^a$ as follows:

$$\begin{aligned} \frac{\partial c_{ij}}{\partial p_i^d}(q, x_{ij}) &= 2(q - p_i^d)^T, \quad i \in \mathcal{C} \\ \frac{\partial c_{ij}}{\partial p_j^a}(q, x_{ij}) &= -2\zeta_{ij}(q, p_j^a)(q - p_j^a)^T \end{aligned} \quad (20)$$

where $\zeta_{ij}(q, p_j^a) = \gamma_{ij}^2 + \frac{r_i \gamma_{ij}}{\|q - p_j^a\|}$. By substituting (20) with $q = \xi_j^{\mathcal{C}}$ into (19) and noting that the parameter λ_{ij}^* is nonnegative, we can obtain an almost robust optimal defense strategy for defender i in coalition \mathcal{C} given by:

$$\pi_i^d(x_j^{\mathcal{C}}) = v_{i, \max}^d \mathcal{N}(\xi_j^{\mathcal{C}} - p_i^d), \quad i \in \mathcal{C} \quad (21)$$

for $x_j^{\mathcal{C}} \in \mathcal{D}'$ such that the convex program (17) has a unique solution. Moreover, it can be shown that the uniqueness of the solution to (17) is guaranteed as long as $\Phi_j^{\mathcal{C}}$ remains positive.

Proposition 3 (Solution Uniqueness): For each joint state $x_j^{\mathcal{C}}$ within the region defined by

$$\mathcal{D}_j^{\mathcal{C}} = \{x_j^{\mathcal{C}} \in \mathcal{D}^{|\mathcal{C}|+1} \mid \Phi_j^{\mathcal{C}}(x_j^{\mathcal{C}}) > 0\}$$

the convex program (17) has a unique solution.

Proof: See Appendix C. ■

We are now ready to present the main result of this section, which asserts that the almost robust optimal defense strategy given by (21) guarantees a win for the coalition once the joint state $x_j^{\mathcal{C}}$ lies within the region $\mathcal{D}_j^{\mathcal{C}}$.

Theorem 1 (Defense-Winning Strategy): For any initial joint state within the region $\mathcal{D}_j^{\mathcal{C}}$, the coalition \mathcal{C} is ensured to win against attacker j under the defense strategy (21), irrespective of any admissible attack strategies.

Proof: In light of Proposition 2, inserting (19) along with (20) and (21) into (18) reveals that for almost every $x_j^{\mathcal{C}} \in \mathcal{D}_j^{\mathcal{C}}$,

$$\begin{aligned} \dot{\Phi}_j^{\mathcal{C}} &= \sum_{i \in \mathcal{C}} 2\lambda_{ij}^* v_{i, \max}^d (\xi_j^{\mathcal{C}} - p_i^d)^T \mathcal{N}(\xi_j^{\mathcal{C}} - p_i^d) \\ &\quad - \sum_{i \in \mathcal{C}} 2\lambda_{ij}^* \zeta_{ij}(\xi_j^{\mathcal{C}}, p_j^a) (\xi_j^{\mathcal{C}} - p_j^a)^T u_j^a \\ &\geq \sum_{i \in \mathcal{C}} 2v_{i, \max}^d \lambda_{ij}^* (\|\xi_j^{\mathcal{C}} - p_i^d\| - \gamma_{ij} \|\xi_j^{\mathcal{C}} - p_j^a\| - r_i) \\ &\geq 0 \end{aligned}$$

where the first and second inequalities hold due to $\|u_j^a\| \leq v_{j, \max}^a$ and $\xi_j^{\mathcal{C}} \in \Omega_j^{\mathcal{C}}(x_j^{\mathcal{C}})$, respectively. As such, $\Phi_j^{\mathcal{C}}(x_j^{\mathcal{C}}(t))$ is

non-decreasing over the time interval $[0, t_f)$. This implies that $\Phi_j^C(x_j^C(t)) \geq \Phi_j^C(x_j^C(0)) > 0$ for all $t \in [0, t_f)$, which in turn completes the proof, as established by Lemma 1. ■

Remark 2 (Maximum Defense-Winning Region): The defense-winning region \mathcal{D}_j^C is *maximum* in the sense that \mathcal{D}_j^C contains all initial joint states for which the coalition \mathcal{C} can assuredly win against attacker j . This is because if an initial joint state $x_j^C(0)$ is not in \mathcal{D}_j^C , then it will lead to $\Phi_j^C(x_j^C(0)) = 0$ according to the definition of \mathcal{D}_j^C . This implies that attacker j can safely reach the target set as stated by Lemma 1. Therefore, the outcome of a single-attack multi-defender reach-avoid game can be fully determined by checking whether the current joint state lies within the defense-winning region \mathcal{D}_j^C .

D. Dual-Mode Switching Defense Coordination

We have identified a region \mathcal{D}_j^C of joint states within which the almost robust optimal defense strategy (21) ensures victory for the coalition. This defense strategy relies on the solution of the convex program (17), which typically does not guarantee solution uniqueness for joint states outside \mathcal{D}_j^C . In real-world scenarios, as the attack strategy is unknown, it would be advantageous for the defense strategy to handle any joint state, not just those within the region \mathcal{D}_j^C . By doing so, the chances of winning for the coalition against non-optimal attack strategies are increased. In the remainder of this section, we focus on utilizing the concept of SRS to extend the defense strategy to cover the entire joint state space.

We start by proposing a novel objective function specifically designed for joint states outside the region \mathcal{D}_j^C . The single-attack objective function Φ_j^C is not suitable for this purpose, as it cannot distinguish between joint states that are not in \mathcal{D}_j^C , resulting in zero values for all such joint states. Given that an intelligent attacker tends to reach the target set safely and rapidly, and the intersection between the SRS and the target set is nonempty for $x_j^C \notin \mathcal{D}_j^C$, the objective function is defined as the minimum squared distance between the attacker's position and the intersection between the SRS and the target set:

$$\bar{\Phi}_j^C(x_j^C) = \min_{q \in \Omega_j^C(x_j^C) \cap \mathcal{G}} \|q - p_j^a\|^2. \quad (22)$$

The convexity of the SRS enables the determination of $\bar{\Phi}_j^C(x_j^C)$ through the solution of the parametric convex program:

$$\begin{aligned} \min_{q \in \mathbb{R}^n} \quad & \|q - p_j^a\|^2 \\ \text{s.t.} \quad & c_{ij}(q, x_{ij}) \leq 0, \quad \forall i \in \mathcal{C} \\ & g_l(q) \leq 0, \quad \forall l \in \mathcal{I}_G. \end{aligned} \quad (23)$$

The uniqueness of the solution to (23) is guaranteed since the projection of p_j^a onto the convex set $\Omega_j^C(x_j^C) \cap \mathcal{G}$ is unique.

The objective function $\bar{\Phi}_j^C$ is then employed to derive a defense strategy for which $x_j^C \notin \mathcal{D}_j^C$. Based on the definition of $\bar{\Phi}_j^C$, the goal of the coalition is to robustly maximize $\bar{\Phi}_j^C$ over time, which can be accomplished by robustly maximizing the time derivative of $\bar{\Phi}_j^C$. To achieve this, we need to determine the gradient of $\bar{\Phi}_j^C$ with respect to the position of each defender in the coalition. Analogous to Proposition 2, it

Algorithm 1: Dual-Mode Switching Defense Coordination

Data: Positions of defenders p_i^d , $i \in \mathcal{C}$ and attacker p_j^a
Result: Defender inputs u_i^d , $i \in \mathcal{C}$
for each defender $i \in \mathcal{C}$ **do**
 $\Phi_j^C, \xi_j^C \leftarrow$ Optimal value and solution of (17) with (\mathcal{C}, j)
 if $\Phi_j^C > 0$ **then**
 $u_i^d \leftarrow v_{i, \max}^d \mathcal{N}(\xi_j^C - p_i^d)$
 else
 $\bar{\xi}_j^C \leftarrow$ Solution to (23) with (\mathcal{C}, j)
 $u_i^d \leftarrow v_{i, \max}^d \mathcal{N}(\bar{\xi}_j^C - p_i^d)$
 end
end

can be shown that for almost every $x_j^C \notin \mathcal{D}_j^C$, there is a set of nonnegative constants μ_{ij}^* , $i \in \mathcal{N}$, such that

$$\begin{aligned} \frac{\partial \bar{\Phi}_j^C}{\partial p_i^d} &= \mu_{ij}^* \frac{\partial c_{ij}}{\partial p_i^d}(\bar{\xi}_j^C, x_{ij}), \quad \forall i \in \mathcal{C} \\ \frac{\partial \bar{\Phi}_j^C}{\partial p_j^a} &= \sum_{i \in \mathcal{C}} \mu_{ij}^* \frac{\partial c_{ij}}{\partial p_j^a}(\bar{\xi}_j^C, x_{ij}) - 2(\bar{\xi}_j^C - p_j^a)^T \end{aligned} \quad (24)$$

where $\bar{\xi}_j^C$ is the unique solution to the convex program (23). The proof of (24), owing to its similarity to that of Proposition 2, can be found in Appendix B. Considering the almost everywhere holding of (24), substituting (20) with $q = \bar{\xi}_j^C$ into (24) yields an almost robust optimal defense strategy for $x_j^C \notin \mathcal{D}_j^C$:

$$p_i^d(x_j^C) = v_{i, \max}^d \mathcal{N}(\bar{\xi}_j^C - p_i^d), \quad \forall i \in \mathcal{C}. \quad (25)$$

This defense strategy, together with the defense strategy (21) for $x_j^C \in \mathcal{D}_j^C$, constitutes a dual-mode switching defense strategy applicable to the entire joint state space. The proposed algorithm for coordinating the defense against a single attacker is outlined in Algorithm 1.

Remark 3 (Almost-Optimal Waypoint for Defense Coordination): Algorithm 1 suggests that the n -dimensional vector defined by

$$\tilde{\xi}_j^C = \begin{cases} \xi_j^C, & x_j^C \in \mathcal{D}_j^C \\ \bar{\xi}_j^C, & \text{otherwise} \end{cases} \quad (26)$$

which is obtained by solving the convex program (17) or (23), serves as an almost-optimal waypoint for the coalition. This waypoint provides a reference point for the defenders in the coalition to coordinate their movements, depending on whether the joint state lies within the region \mathcal{D}_j^C or not, as illustrated in Fig. 3. By following the almost-optimal waypoint, the coalition can effectively adapt their defense strategy to defend against a single attacker.

Remark 4 (Individual Attack Strategy): As a byproduct of our analysis, we can also derive a strategy for the single attacker. Contrary to the defenders' goal, the attacker seeks to minimize Φ_j^C robustly for $x_j^C \in \mathcal{D}_j^C$, and $\bar{\Phi}_j^C$ robustly for $x_j^C \notin \mathcal{D}_j^C$. Employing a similar approach to that used in the

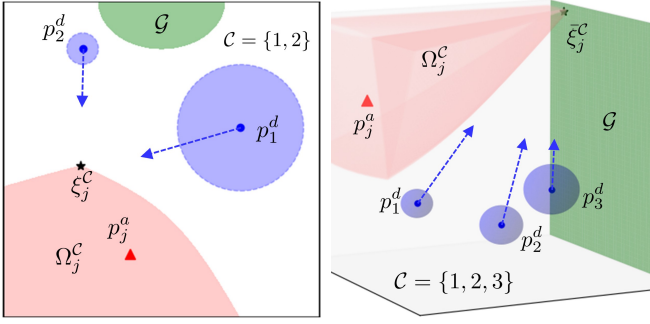


Fig. 3. Defense coordination in both 2D and 3D cases. On the left, the almost-optimal waypoint ξ_j^C (star) represents the point within the SRS Ω_j^C that is closest to the target set \mathcal{G} . On the right, the almost-optimal waypoint ξ_j^C (star) signifies the point within the intersection of the SRS Ω_j^C and the target set \mathcal{G} that is closest to the attacker. Both almost-optimal waypoints offer intuitive and effective reference points for the coalition to intercept the attacker in various scenarios.

derivation of the defense strategy, we arrive at the following attack strategy:

$$\pi_j^a(x_j^C) = v_{j,\max}^a \mathcal{N}(\tilde{\xi}_j^C - p_j^a) \quad (27)$$

where $\tilde{\xi}_j^C$, defined as (26), also serves as an almost-optimal waypoint for the attacker. The detailed derivation is omitted in this paper, as our primary focus lies on the defense perspective.

IV. DEFENSE ALLOCATION FOR MULTIPLE ATTACKERS

In this section, we delve into the dynamic problem of allocating coalitions to multiple attackers. Building upon our previous results on defense coordination for single-attacker scenarios, we formulate the defense allocation problem as a joint state-dependent integer linear program (ILP), but solving this ILP in real-time may become computationally infeasible as the agent size grows. To address this issue, we propose an alternative solution that integrates two key components: the Hierarchical Integer Linear Programming (HILP) method and the Monotonic Defense Enhancement Allocation (MDEA) algorithm. The HILP method iteratively constructs a hierarchy based on the concepts of active defense sets and irreducibility, leading to a computationally efficient suboptimal solution. The MDEA algorithm then incorporates this suboptimal solution while enforcing a monotonicity constraint, ensuring that the expected number of attackers that fail to reach the target set remains non-decreasing over time.

A. Integer Linear Program Formulation

Following the classical taxonomy of multirobot task allocation proposed by Gerkey et al. [25], the defense allocation problem can be categorized as a single-task robot, multirobot task, and instantaneous assignment problem. Under the current joint state, each defender can defend against at most one attacker at a time, each attacker can be simultaneously guarded by multiple defenders, and the assignment only concerns the present moment. To represent the assignment, a binary matrix called the assignment matrix $\mathcal{A} = (a_{ij})_{N \times M}$ is used, where the entry $a_{ij} = 1$ if attacker j is assigned to defender i , and 0 otherwise. In addition, since all defenders are single-task, the

assignment matrix must respect the *conflict-free* constraint, i.e., the row sum of the assignment matrix should not exceed 1.

To better model the effect of each coalition-attacker pair on the defense performance, we introduce an alternative matrix representation. Let $\mathcal{C}_k, k = 1, \dots, \tilde{N}$ be the list of all different coalitions in which $\tilde{N} = 2^N - 1$. We define the *coalition assignment matrix* to be $\Theta = (\theta_{kj})_{\tilde{N} \times M}$ such that

$$\theta_{kj} \in \{0, 1\}, \forall k = 1, \dots, \tilde{N}, j = 1, \dots, M \quad (28)$$

and $\theta_{kj} = 1$ if attacker j is allocated to coalition \mathcal{C}_k . The coalition assignment matrix Θ inherently induces an assignment matrix \mathcal{A} through the linear transformation:

$$\mathcal{A} = \mathcal{B}\Theta \quad (29)$$

where $\mathcal{B} = (b_{ik})_{N \times \tilde{N}}$ denotes the *incidence matrix* representing the binary relationship between defenders and coalitions. Specifically, $b_{ik} = 1$ if $i \in \mathcal{C}_k$ and 0 otherwise. To maintain the single-task property, the conflict-free constraint is defined through the induced assignment matrix as

$$\sum_{j=1}^M \sum_{k=1}^{\tilde{N}} b_{ik} \theta_{kj} \leq 1, \forall i = 1, \dots, N. \quad (30)$$

Additionally, the *redundancy-free* constraint is imposed on Θ :

$$\sum_{k=1}^{\tilde{N}} \theta_{kj} \leq 1, \forall j = 1, \dots, M \quad (31)$$

ensuring that each attacker is assigned to at most one coalition.

We now present an objective function incorporating decision variables as elements of the coalition assignment matrix. Recalling Theorem 1, if $\Phi_j^{C_k} > 0$ at the joint state $x_j^{C_k}$, an admissible defense strategy for \mathcal{C}_k exists that prevents attacker j from reaching the target set. In light of this, we designate (\mathcal{C}_k, j) as a *feasible* coalition-attacker pair at $x_j^{C_k}$ if $\Phi_j^{C_k}(x_j^{C_k}) > 0$. In line with the payoff function given in (12), the *reward* for assigning attacker j to coalition \mathcal{C}_k , denoted by w_{kj} , is set as 1 if (\mathcal{C}_k, j) is feasible and attacker j is active, and 0 otherwise, i.e.,

$$w_{kj}(x_j) = \rho_j(x_j) \mathcal{N}(\Phi_j^{C_k}(x_j^{C_k}))$$

with ρ_j given in (10). Subsequently, the objective function, depending on the choice of a coalition assignment matrix Θ at a given joint state x , is defined as the total sum of the rewards of all assigned coalition-attacker pairs:

$$\Gamma(\Theta, x) = \sum_{k=1}^{\tilde{N}} \sum_{j=1}^M w_{kj}(x_j) \theta_{kj}. \quad (32)$$

We refer to Γ as the *multi-attack objective function*, which signifies the expected number of attackers that will be unable to access the target set from the current joint state. The reason behind this objective function is that it enables the assessment of defense performance in multi-attack scenarios.

Lemma 2 (Defense Performance Assessment): Let π^d be an admissible defense strategy associated with time-dependent coalition assignment matrices $\Theta(\cdot)$ that consistently satisfy

constraints (28), (30), and (31). Suppose there exists a time instant $t_0 \geq 0$, such that for all admissible attack strategies,

$$\Gamma(\Theta(t), x(t)) + N_c(t) \geq M_c \quad (33)$$

holds over the time interval $[t_0, t_f]$, where $N_c(t)$ is the number of captured attackers up to time t , and M_c is a positive integer. Then, the payoff function J under the defense strategy π^d is bounded by $M - M_c$, i.e.,

$$J(x(0), \pi^d, \pi^a) \leq M - M_c$$

for any admissible attack strategy π^a .

Proof: Let $N_e(t)$ denote the number of attackers that have entered the target set up to time t . At time t , each attacker must be either captured, active, or have entered the target set. Hence, we have $M = N_e(t) + M_a(t) + N_c(t)$. Since the multi-attack objective function Γ only concerns active attackers, it follows that $\Gamma(\Theta(t), x(t)) \leq M_a(t)$. Combining this with inequality (33) yields $M_c \leq \Gamma(\Theta(t), x(t)) + N_c(t) \leq M_a(t) + N_c(t)$ for all $t \in [t_0, t_f]$, implying that $N_e(t) \leq M - M_c$ for all $t \in [t_0, t_f]$. Consequently, based on the definition of the payoff function, we obtain $J(x(0), \pi^d, \pi^a) = N_e(t_f) \leq M - M_c$. ■

Remark 5 (Online Maximization and Monotonicity Constraint): Lemma 2 implies that one way to minimize the payoff function J , against any admissible attack strategies, is to maximize the multi-attack objective function Γ with respect to the coalition assignment matrix Θ at each joint state x . This leads to the following integer linear program (ILP) for the multi-attack defense allocation problem along the joint state trajectory:

$$\begin{aligned} \max_{\Theta} \quad & \Gamma(\Theta, x) \\ \text{s.t.} \quad & (28), (30), (31). \end{aligned} \quad (34)$$

Furthermore, to ensure overall defense performance, Lemma 2 highlights the significance of maintaining a robustly positively invariant superlevel set for the function $\Gamma + N_c$ with a level $M_c > 0$. Here, the value $\Gamma(\Theta(t), x(t)) + N_c(t)$ represents the expected number of attackers that fail to reach the target set at time t . A sufficient condition for preserving the superlevel set property is to impose the monotonicity constraint, given by:

$$\begin{aligned} & \Gamma(\Theta(t_l), x(t_l)) + N_c(t_l) \\ & \geq \Gamma(\Theta(t_{l-1}), x(t_{l-1})) + N_c(t_{l-1}), \quad \forall l = 1, \dots, L \end{aligned} \quad (35)$$

where t_l , $l = 0, \dots, L$ are the allocation times with $t_0 = 0$. It should be noted that the optimal solution to the ILP (34) automatically satisfies the monotonicity constraint (35).

Despite solving the ILP (34) provides an optimal solution to the defense allocation problem, it entails a substantial computational burden, particularly as the number of agents increases. This is mainly due to the vast amount of possible coalition-attack pairs, which not only leads to a large-scale ILP, but more importantly requires considerable computational effort to determine the multi-attack objective function. In the case of N defenders and M_a active attackers, there are $\bar{N}M_a$ possible coalition-attacker pairs, implying that the same amount of convex programs of the form (17) need to be calculated to specify the corresponding rewards. To alleviate the computational burden, we propose a heuristic algorithm

for the ILP (34) in Section IV-C to generate a suboptimal solution, which will then be fed into an allocation algorithm to ensure the monotonicity constraint (35) in Section IV-D. In particular, prior to detailing the heuristic algorithm, we will derive two critical components in the next section, which together construct a hierarchy that facilitates the generation of a suboptimal solution for the ILP (34).

B. Active-Defense Set and Irreducibility

The optimal solution to the ILP (34) tends to favor feasible coalition-attacker pairs comprising smaller coalitions. On one hand, the multi-attack objective function is influenced only by feasible coalition-attacker pairs, as the reward for an infeasible pair is zero. On the other hand, smaller coalitions are less likely to violate the conflict-free constraint (30), and thus more likely to contribute positively to the multi-attack objective function. As a result, the key to striking a balance between optimality and efficiency in solving the ILP (34) is to identify as many feasible sub-pairs of coalition-attacker pairs with small amounts of defenders as possible while keeping the computational cost low. Here, a *sub-pair* of a coalition-attacker pair refers to a subset of the coalition that is also paired with the same attacker. To this end, we will focus on seeking feasible sub-pairs of a coalition-attacker pair from the aspects of optimality and efficiency in the subsequent analysis.

As a point of departure, we revisit the convex program (17) subject to a feasible coalition-attacker pair (\mathcal{C}, j) . As shown in Theorem 1, the vector $\xi_j^{\mathcal{C}}$ extracted from the solution to (17) establishes an almost-optimal waypoint for the coalition \mathcal{C} , which must lie on the boundary of the SRS $\Omega_j^{\mathcal{C}}$. Moreover, owing to the convexity of the SRS, some of the inequality constraints $c_{ij}(q, x_{ij}) \leq 0$, $i \in \mathcal{C}$ must be active at $q = \xi_j^{\mathcal{C}}$. As such, we can define an index set of defenders through an active set in the convex program (17) that incorporates the almost-optimal waypoint $\xi_j^{\mathcal{C}}$.

Definition 2 (Active-Defense Set): Suppose the coalition-attacker pair (\mathcal{C}, j) is feasible at the joint state $x_j^{\mathcal{C}}$. The *active-defense set* (ADS) $\Lambda_j^{\mathcal{C}}(x_j^{\mathcal{C}})$ for (\mathcal{C}, j) is the active set of the inequality constraints $c_{ij}(q, x_{ij}) \leq 0$, $i \in \mathcal{C}$ in (17) at the almost-optimal waypoint $\xi_j^{\mathcal{C}}$, i.e.,

$$\Lambda_j^{\mathcal{C}}(x_j^{\mathcal{C}}) = \{i \in \mathcal{C} \mid c_{ij}(\xi_j^{\mathcal{C}}, x_{ij}) = 0\}. \quad (36)$$

The construction of the ADS does not necessitate the computation of any additional convex programs. This is because the feasibility of the coalition-attacker pair has already been verified using a convex program of the form (17), and the almost-optimal waypoint can be determined as a byproduct of this computation. It is worth noting that the ADS concept indeed provides a proximity-based method for obtaining a specific sub-pair, which is associated with both locations of the attacker and the target set, as illustrated in Fig. 4. Furthermore, it can be shown that such a sub-pair inherits the feasibility of the original coalition-attacker pair.

Proposition 4 (Feasibility): If the coalition-attacker pair (\mathcal{C}, j) is feasible at the joint state $x_j^{\mathcal{C}}$, then the sub-pair $(\Lambda_j^{\mathcal{C}}, j)$ is also feasible at the corresponding joint state.

Proof: See Appendix D. ■

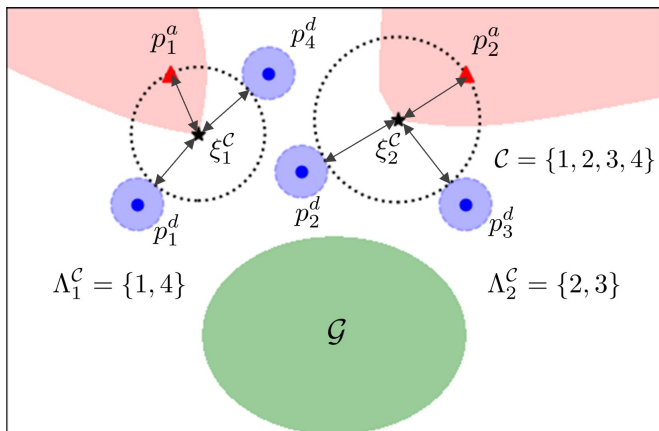


Fig. 4. Geometric interpretation of the ADS in a 2D domain for the case of $\gamma_{ij} = 1$. In this case, the ADS Λ_j^C is the set of defender indices such that the capture region for each defender $i \in \Lambda_j^C$ (illustrated as a blue disk) is tangent to the dashed circle of radius $\|\xi_j^C - p_j^a\|$ centered at the almost-optimal waypoint ξ_j^C .

We turn to look at how to generate feasible sub-pairs of a sufficiently small scale. While the ADS allows for feasible sub-pair generation without incurring additional computational effort, the resulting sub-pair size may not be minimum with respect to feasibility. In other words, the sub-pair may include redundant defenders that could be removed without affecting the feasibility of the sub-pair. To precisely quantify the redundancy, we introduce the following definition.

Definition 3 (Irreducibility): A feasible coalition-attacker pair (C, j) is said to be *irreducible* at a joint state x_j^C if there is no proper subset C' of C such that (C', j) is feasible.

Given a feasible coalition-attacker pair (C, j) , we can develop an iterative procedure to generate all irreducible sub-pairs. The process commences by evaluating size-1 subsets of C . If $|C| = 1$, (C, j) is inherently deemed irreducible, and the process terminates. Otherwise, we check each size-1 subset C' for irreducibility by confirming whether $\Phi_j^{C'} > 0$. Then, we remove the element of C' from C for which (C', j) is irreducible, forming a new set $C_r^{(1)}$. If $|C_r^{(1)}| \leq 1$, all irreducible sub-pairs have been identified, and the process ends. In case further iterations are required, we repeat with all size- l subsets of $C_r^{(l-1)}$ for $l = 2, \dots, |C|$, where $C_r^{(l)}$ is analogously defined by removing elements from $C_r^{(l-1)}$. The procedure continues until either $|C_r^{(l)}| \leq l$ or $|C| = l$ at the iteration l . Moreover, the number of iterations can be reduced by noting that the cardinality of the coalition for any irreducible sub-pair is upper bounded by the dimension of the domain.

Proposition 5 (Upper Bounded Cardinality): In an n -dimensional domain, if the coalition-attacker pair (C, j) is irreducible, then C has cardinality no greater than n .

Proof: See Appendix E. ■

We summarize our findings of identifying irreducible sub-pairs of a feasible coalition-attacker pair in Algorithm 2. It should be emphasized that when solving the ILP (34), we can focus on irreducible coalition-attacker pairs rather than all possible pairs. This is because replacing a coalition-attacker

Algorithm 2: Irreducible Sub-Pairs of (C, j)

Data: Positions $p_i^d \in \mathbb{R}^n$, $i \in C$ and $p_j^a \in \mathbb{R}^n$

Result: Set \mathcal{P}

Initialization: $\mathcal{P} \leftarrow \emptyset$, $C_r \leftarrow C$

```

for  $i = 1$  to  $n$  do
  if  $|C_r| < i$  then
    break
  else if  $|C| = i$  then
    Put  $(C, j)$  in  $\mathcal{P}$ 
    break
  else
    forall  $C' \subset C_r$  with  $|C'| = i$  do
       $\Phi_j^{C'} \leftarrow$  Optimal value of (17) s.t.  $(C', j)$ 
      if  $\Phi_j^{C'} > 0$  then
        Put  $(C', j)$  in  $\mathcal{P}$ 
        Remove the elements of  $C'$  from  $C_r$ 
      end
    end
  end
end

```

pair with one of its irreducible sub-pairs will not affect the optimal value of the multi-attack objective function. In general, Algorithm 2 can lower the number of convex programs needed to determine the multi-attack objective function. However, directly using the concept of irreducibility could lead to heavy computational loads. For instance, computing all irreducible sub-pairs in the worst-case scenario requires up to compute \tilde{N} convex programs for a coalition-attacker pair (\mathcal{N}, j) . To improve computational efficiency, a more effective approach would be to combine the concept of irreducibility with that of the ADS.

C. Hierarchical Integer Linear Programming

We now exhibit the integration of the ADS and irreducibility concepts to establish the first level of the hierarchy for the ILP (34). Our approach initiates by checking coalition-attack pairs of the form (\mathcal{N}, j) and only focusing on feasible ones. The proximity-based sub-pair $(\Lambda_j^{\mathcal{N}}, j)$ is then taken into account, where $\Lambda_j^{\mathcal{N}}$ is the ADS for the feasible pair (\mathcal{N}, j) . Finally, irreducible sub-pairs of $(\Lambda_j^{\mathcal{N}}, j)$ are selected to refine the multi-attack objective function Γ . As a result, we assign the highest priority to coalition-attacker pairs (C, j) that are irreducible and have C as a subset of $\Lambda_j^{\mathcal{N}}$. Compared to directly prioritizing all irreducible sub-pairs of (\mathcal{N}, j) , this method reduces the potential computational challenges while offering a considerable amount of feasible sub-pairs.

After specifying the first hierarchy level, we can derive a suboptimal solution to the ILP (34). Let Ξ_1 denote the first priority set that contains all coalition-attacker pairs with the highest priority. In the case where Ξ_1 is empty, no feasible coalition-attacker pairs exist, and the ILP solution simply corresponds to a zero coalition assignment matrix. To confine the selection of coalition-attacker pairs solely to those

within Ξ_1 , we impose the following constraint on the decision variables:

$$\theta_{kj} = 0, \forall (\mathcal{C}_k, j) \notin \Xi_1. \quad (37)$$

By resolving the ILP (34) with the additional constraint (37), we attain a suboptimal solution denoted as Θ_1 , which provides a lower bound on the optimal value of the multi-attack objective function. In order to evaluate Θ_1 , we define two index sets $\mathcal{N}_r^{(1)}$ and $\mathcal{M}_r^{(1)}$ in which $\mathcal{N}_r^{(1)}$ contains the indices of defenders that remain unassigned to any attacker based on Θ_1 , and $j \in \mathcal{M}_r^{(1)}$ if Θ_1 omits attacker j and (\mathcal{N}, j) is feasible. If either $\mathcal{N}_r^{(1)}$ or $\mathcal{M}_r^{(1)}$ is empty, there are no more available coalition-attacker pairs and further steps are not needed.

The above procedure can be iteratively applied, if possible, to improve the suboptimal solution. At iteration $l \geq 2$, the l -th priority set Ξ_l is formed by identifying all irreducible coalition-attacker pairs (\mathcal{C}, j) for which \mathcal{C} is contained in the ADS for a feasible $(\mathcal{N}_r^{(l-1)}, j)$ and $j \in \mathcal{M}_r^{(l-1)}$. The decision variables are then restricted to Ξ_l through the binary constraint:

$$\theta_{kj} = 0, \forall (\mathcal{C}_k, j) \notin \Xi_l \quad (38)$$

resulting in a subproblem of the original ILP (34):

$$\begin{aligned} \max \quad & \Gamma(\Theta, x) \\ \text{s.t.} \quad & (28), (30), (31), (38). \end{aligned} \quad (39)$$

Having a solution to the subproblem (39), represented by Θ_l , the suboptimal solution to the ILP (34) is updated by adding Θ_l to the previous suboptimal solution, leading to

$$\Theta_{\text{HILP}} = \sum_{k=1}^l \Theta_k.$$

The procedure terminates at the l th iteration when Ξ_l is empty or one of the index sets $\mathcal{N}_r^{(l)}$ and $\mathcal{M}_r^{(l)}$ is empty, where $\mathcal{N}_r^{(l)}$ and $\mathcal{M}_r^{(l)}$ are obtained by excluding the indices related to Θ_l from $\mathcal{N}_r^{(l-1)}$ and $\mathcal{M}_r^{(l-1)}$, respectively.

In summary, our approach to solving the ILP (34) is outlined in Algorithm 3, which strikes a balance between optimality and efficiency, as demonstrated by the subsequent proposition.

Proposition 6 (Optimality-Efficiency Tradeoff): Algorithm 3 possesses two key properties:

1) (Optimality) If \mathcal{M}_r is empty after the first iteration, then the suboptimal solution Θ_{HILP} is an optimal solution to the ILP (34).

2) (Efficiency) If the cardinality of the ADS for each (\mathcal{N}_r, j) in each iteration is at most n , then the total number of calculations for the convex program of the form (17) is less than $2^{n-1}M_a(1 + M_a)$.

Proof: See Appendix F. ■

The assumptions made in Proposition 6 for Algorithm 3 are satisfied in many practical scenarios. For instance, if the ADSs $\Lambda_j^{\mathcal{N}_r}$ for the coalition-attacker pair (\mathcal{N}, j) , $j \in \mathcal{M}_a$ are mutually disjoint, then the set \mathcal{M}_r becomes empty after the first iteration and the suboptimal solution $\tilde{\Theta}$ is optimal for the ILP (34). Such a scenario commonly arises when the attackers are sparsely distributed relative to the defenders. Furthermore, empirical results indicate that the cardinality of

Algorithm 3: Hierarchical Integer Linear Programming

Data: Positions p_i^d , $i \in \mathcal{N}$ and p_j^a , $j \in \mathcal{M}_a$

Result: Coalition assignment matrix Θ_{HILP}

Initialize $\Theta_{\text{HILP}} \leftarrow 0_{\tilde{N} \times M}$, $\mathcal{N}_r \leftarrow \mathcal{N}$, $\mathcal{M}_r \leftarrow \mathcal{M}_a$

while $\mathcal{N}_r \neq \emptyset$ **and** $\mathcal{M}_r \neq \emptyset$ **do**

$\Xi \leftarrow \emptyset$

forall $j \in \mathcal{M}_r$ **do**

$\Phi_j^{\mathcal{N}_r} \leftarrow$ Optimal value of (17) s.t. (\mathcal{N}_r, j)

if $\Phi_j^{\mathcal{N}_r} > 0$ **then**

$\Lambda_j^{\mathcal{N}_r} \leftarrow$ ADS for (\mathcal{N}_r, j)

$\mathcal{P} \leftarrow$ Result of Algorithm 2 s.t. $(\Lambda_j^{\mathcal{N}_r}, j)$

 Put all elements of \mathcal{P} in Ξ

else

 Remove j from \mathcal{M}_r

end

end

if $\Xi = \emptyset$ **then**

break

end

$\Theta \leftarrow$ A solution to the ILP (39) with (38) s.t. Ξ

$\Theta_{\text{HILP}} \leftarrow \Theta_{\text{HILP}} + \Theta$

 Remove all i with $(\mathcal{B}\Theta)(i, :) \neq 0_{1 \times M}$ from \mathcal{N}_r

 Remove all j with $\Theta(:, j) \neq 0_{\tilde{N} \times 1}$ from \mathcal{M}_r

end

the ADSs typically does not exceed the number of defenders. Compared to directly solving the ILP, where the number of calculations for the convex program of the form (17) grows exponentially with the number of defenders, the calculation times for our algorithm do not empirically depend on the number of defenders and are only quadratically dependent on the number of active attackers. Consequently, Algorithm 3 offers a viable alternative for tackling the ILP in large-scale scenarios with many defenders, especially when conventional approaches become computationally infeasible.

D. Monotonic Defense Enhancement Allocation

Once acquiring the suboptimal solution produced by Algorithm 3, we adjust it by incorporating the monotonicity constraint (35). Specifically, we update the coalition assignment matrix at each time step by equating it to the solution derived from Algorithm 3 if the monotonicity constraint (35) is met; otherwise, we retain the updated coalition assignment matrix from the previous step. Note that the number of active attackers may change between two consecutive time steps. As such, we need to set the columns of the previous coalition assignment matrix to zero for those corresponding to attackers captured at the current time step before executing the update. This approach offers the advantage of maintaining the validity of all inequalities in (34) without requiring additional computation of the ILP, thereby reducing the computational effort.

While the above approach effectively integrates the monotonicity constraint (35), it may give rise to undesired oscillatory behaviors in defense allocation. Such oscillations occur when a defender's assignment repeatedly switches between

Algorithm 4: Monotonic Defense Enhancement Allocation

Data: Positions $p_i^d, i \in \mathcal{N}$ and $p_j^a, j \in \mathcal{M}_a$, solution of Algorithm 3 Θ_{HILP} , previous coalition assignment matrix $\tilde{\Theta}^p$, previous index set of active attackers \mathcal{M}_a^p ,

Result: Coalition assignment matrix Θ_{MDEA}

if $\mathcal{M}_a = \emptyset$ **then**
 | **return** $\Theta_{\text{MDEA}} \leftarrow 0_{\tilde{N} \times M}$
end

Part I: Monotonicity constraint enforcement

$\Gamma \leftarrow$ Number of nonzero column vectors in Θ_{HILP}

$\Gamma^p \leftarrow$ Number of nonzero column vectors in $\tilde{\Theta}^p$

if $\Gamma > \Gamma^p - |\mathcal{M}_a^p| + |\mathcal{M}_a|$ **then**

| $\Theta_{\text{MDEA}} \leftarrow \Theta_{\text{HILP}}$

else

| **if** $|\mathcal{M}_a^p| \neq |\mathcal{M}_a|$ **then**

| | **forall** $j \in \mathcal{M}_a^p \setminus \mathcal{M}_a$ **do**

| | | $\tilde{\Theta}^p(:, j) \leftarrow 0_{\tilde{N} \times 1}$

| | **end**

| **end**

| $\Theta_{\text{MDEA}} \leftarrow \tilde{\Theta}^p$

end

$\tilde{\Theta}^p \leftarrow \Theta_{\text{MDEA}}, \mathcal{M}_a^p \leftarrow \mathcal{M}_a$

Part II: Greedy assignment of unassigned defenders

$\mathcal{A} \leftarrow \mathcal{B}\Theta_{\text{MDEA}}$

Put all $i \in \mathcal{N}$ with $\mathcal{A}(i, :) = 0_{1 \times M}$ in \mathcal{N}_r

Put all $j \in \mathcal{M}_a$ with $\mathcal{A}(:, j) = 0_{N \times 1}$ in \mathcal{M}_r

if $\mathcal{M}_r \neq \emptyset$ and $\mathcal{N}_r \neq \emptyset$ **then**

| **forall** $i \in \mathcal{N}_r$ **do**

| | $j_{\min} \leftarrow \arg \min_{j \in \mathcal{M}_r} \|p_i^d - p_j^a\|$

| | (i, j_{\min}) th element of $\mathcal{A} \leftarrow 1$

| **end**

end

$\Theta_{\text{MDEA}} \leftarrow \mathcal{B}^\dagger \mathcal{A}$

two distinct attackers, potentially impairing the system's performance. These oscillations stem from the fact that Algorithm 3 might produce non-unique solutions, leading to the equality in (35) holding. To tackle this issue, we implement a stricter version of the monotonicity constraint (35), updating the coalition assignment matrix only when the inequality constraint (35) is strictly fulfilled. This ensures that we stick to the previous coalition assignment matrix when the equality in (35) holds, thus avoiding oscillations while still enforcing the monotonicity constraint (35).

Our approach to the multi-attack defense allocation problem is summarized in Algorithm 4, which consists of two components. The first component imposes the monotonicity constraint (35) on the solution obtained from Algorithm 3. For the initial step, $\tilde{\Theta}^p$ and \mathcal{M}_a^p are respectively set to Θ_{HILP} and $\mathcal{M}_a^p = \mathcal{M}$. The second part uses a greedy algorithm that allocates each unassigned defender to the nearest unassigned active attacker. This is inspired by the observation that a closer the defender-attacker pair results in a reduced SRS. To achieve this, we first convert the coalition assignment matrix into

the corresponding assignment matrix in terms of the linear equation (29). We then update the assignment matrix using the greedy algorithm and revert it to the coalition assignment matrix through the pseudoinverse of the incidence matrix. The greedy algorithm is computationally efficient and provides a valuable supplement to the first component of Algorithm 4.

We are now able to encode the solution to the multi-attack defense allocation problem into an admissible defense strategy for the multiplayer reach-avoid game. Given the output of Algorithm 4, $\Theta_{\text{MDEA}} = (\theta_{kj})$, we define the assignment rule as follows:

$$\sigma(i) = \begin{cases} j, & i \in \mathcal{C}_k \ \& \ \theta_{kj} = 1 \\ \text{null}, & \forall \theta_{kj} = 0 \end{cases} \quad (40)$$

where null denotes the case of an unassigned defender. For each active attacker $j \in \mathcal{M}_a$, the coalition against attacker j induced by σ is given by:

$$\tilde{\mathcal{C}}_j = \{i \in \mathcal{N} \mid \sigma(i) = j\}.$$

Combining Algorithm 1 with the assignment rule σ as described in (40), we obtain an admissible defense strategy of the form:

$$\tilde{\pi}_i^d(x) = v_{i, \max}^d \mathcal{N}(\xi_{\sigma(i)} - p_i^d), \quad i \in \mathcal{N} \quad (41)$$

where $\xi_j = \tilde{\xi}_j^c$ is the almost-optimal waypoint defined in (26). If a defender is unassigned, its control input is set to zero for the sake of energy saving.

Theorem 2 (Performance-Guaranteed Defense Strategy):

For any initial joint state x_0 , the payoff function J under the defense strategy $\tilde{\pi}^d$ given by (41), and any admissible attack strategy satisfies the following inequality:

$$J(x_0, \tilde{\pi}^d, \pi^a) \leq M - \Gamma(\Theta_{\text{MDEA}}^0, x_0) - N_c(0) \quad (42)$$

where Γ is the multi-attack objective function defined in (32), Θ_{MDEA}^0 is the initial solution of Algorithm 4, and $N_c(0)$ is the number of attackers captured at the initial joint state. Moreover, the function $\Gamma + N_c$ is monotonically non-decreasing along the system trajectory.

Proof: The enforcement of the monotonicity constraint (35) in Algorithm 4 ensures that the sequence $\Gamma(\Theta_{\text{MDEA}}(t_l), x(t_l)) + N_c(t_l)\}_{l=0}^L$ is monotonically non-decreasing. Further, it is noted that $\Gamma(\Theta_{\text{MDEA}}(t), x(t)) + N_c(t)$ remains constant within each time interval $[t_{l-1}, t_l)$, as the assignment of defenders to active attackers is updated only at the time instants t_l . As a result, $\Gamma + N_c$ is non-decreasing. This indicates that the inequality (33) holds with $M_c = \Gamma(\Theta_{\text{MDEA}}^0, x_0) + N_c(0)$, which in turn, according to Lemma 2, leads to the satisfaction of the inequality (42) for the payoff function. ■

Theorem 2 provides a solid assurance that our defense strategy (41) is capable of achieving a performance level no worse than the bound of the payoff function specified in (42) for any initial joint state. Theorem 2 also establishes that the function $\Gamma + N_c$, representing the expected number of attackers that fail to reach the target set, is monotonically non-decreasing over time. This property suggests that the upper bound of the payoff function in (42) becomes progressively tighter as the game progresses, leading to a continuous improvement in

the performance of the proposed strategy. In the next section, we will present empirical results to demonstrate performance enhancement in practical scenarios.

V. SIMULATIONS

In this section, we assess the performance and efficiency of our proposed defense coordination and allocation algorithms through a series of simulated experiments. All algorithms are written in python, with convex programs and ILP implemented using the CVXPY solver [26]. We conduct the experiments on an Ubuntu 20.04 operating system equipped with an i9-10900 5.2 GHz CPU and 32 GB RAM, featuring 10 physical cores and 20 threads. To demonstrate the effectiveness of our approach, we benchmark our algorithms against current state-of-the-art algorithms in both 2D and 3D scenarios. Initially, we examine the Dual-Mode Switching Defense Coordination (DMSDC) algorithm (Algorithm 1), which serves as the basis for subsequent experiments with the monotonic defense enhancement allocation (MDEA) algorithm (Algorithm 4). Furthermore, to demonstrate the applicability of our algorithms in practical settings, we extend our evaluation to a more realistic simulation environment utilizing Gazebo and the Robot Operating System (ROS) [27].

A. Single-Attack Defense Coordination

We first evaluate the performance of our proposed algorithm (Algorithm 1) in a single-attack defense coordination problem. Our approach is compared with two existing strategies: the multi-agent pursuit-defense strategy presented in [21] for a 2D scene and the optimal defense strategy introduced in [15] for a 3D scene. We conduct simulations in a 2D rectangular domain of $[-5, 5]^2$ with a unit circle as the target set, and a 3D box domain of $[-5, 5]^3$ with the origin as the target set. To examine the effectiveness of our approach in guaranteeing the coalition's win under various initial joint states, we perform 2000 randomized simulations with different numbers of defenders and capture radii for both the 2D and 3D scenarios. To ensure a fair comparison, we adopt the attack strategy given in (27) and set the maximum speed ratios to 1. The simulation outcomes are classified into four categories based on whether the coalition wins the game:

- True Positive: The percentage of cases where both methods successfully capture the attacker.
- False Negative: The percentage of cases where our method succeeds while the comparison method fails to capture the attacker.
- False Positive: The percentage of cases where our method fails while the comparison method succeeds in capturing the attacker.
- True Negative: The percentage of cases where both methods fail in capturing the attacker.

Table I showcases the 2D simulation results, which highlight the superior performance of our proposed algorithm over the multi-agent pursuit-defense strategy. Notably, our algorithm captures the attacker in 7.1% to 22.4% more instances than

TABLE I
SIMULATION RESULTS OF A 2D MULTI-DEFENDER SINGLE-ATTACKER REACH-AVOID GAME.

Defender Number	Capture Radius	True Positive	False Negative	False Positive	True Negative
2	0.5	25.6%	7.1%	0%	67.3%
3	0.5	33.0%	10.0%	0%	57.0%
2	3.0	33.9%	18.8%	0%	47.3%
3	3.0	41.6%	22.4%	0%	36.0%

the multi-agent pursuit-defense strategy, without any occurrences where our algorithm fails while the multi-agent pursuit-defense strategy prevails. Interestingly, as the capture radius increases, our algorithm records a higher percentage of false negatives. This observation can be attributed to the fact that the Voronoi diagram employed in the multi-agent strategy does not inherently account for nonzero capture radii, whereas our algorithm exploits the safe-reachable set of the attacker to devise a more effective defense coordination strategy. Moreover, we note that when the number of defenders increases from 2 to 3, both capture radius scenarios exhibit a higher percentage of false negatives. This result arises from the multi-agent pursuit-defense strategy utilizing only one defender for defense, with the remaining defenders acting as pursuers. In contrast, our algorithm capitalizes on the collective strength of multiple defenders to achieve overall coordination.

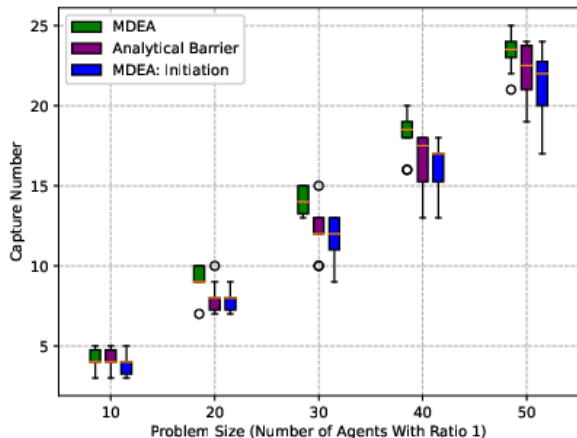
TABLE II
SIMULATION RESULTS OF A 3D MULTI-DEFENDER SINGLE-ATTACKER REACH-AVOID GAME.

Defender Number	Capture Radius	True Positive	False Negative	False Positive	True Negative
2	0.1	66.5%	0.9%	0%	32.6%
3	0.1	72.2%	1.6%	0%	26.2%
2	2.0	84.3%	7.3%	0%	8.4%
3	2.0	81.6%	13.6%	0%	5.2%

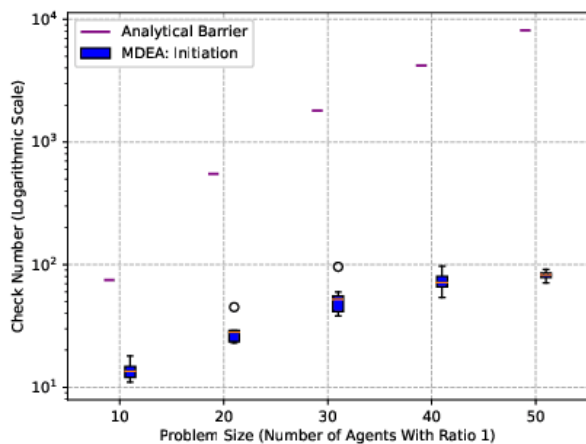
On the other hand, the 3D simulation results displayed in Table II indicate that our proposed algorithm outperforms the optimal defense strategy. Specifically, our algorithm captures the attacker in up to 13.6% more instances than the optimal defense strategy when the capture radius is 2, and there are no cases in which our algorithm fails while the optimal defense strategy succeeds. It should be emphasized that the optimal defense strategy is designed for cases with zero capture radii; consequently, the performance of our algorithm closely aligns with the optimal defense strategy when the capture radius is near zero, which in turn demonstrates the optimality of our approach. Additionally, our algorithm exhibits better performance as the number of defenders increases, similar to our 2D comparison. This improvement is due to the optimal defense strategy in [15] focusing solely on scenarios with one or two defenders, whereas our approach accommodates multiple defenders.

B. Multiple-Attack Defense Allocation

We next examine the performance and efficiency of our proposed MDEA algorithm (Algorithm 4) for the multi-attack defense allocation problem. We compare our approach to two



(a)

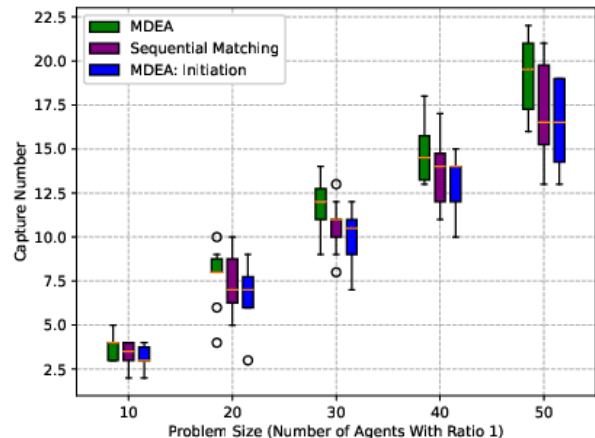


(b)

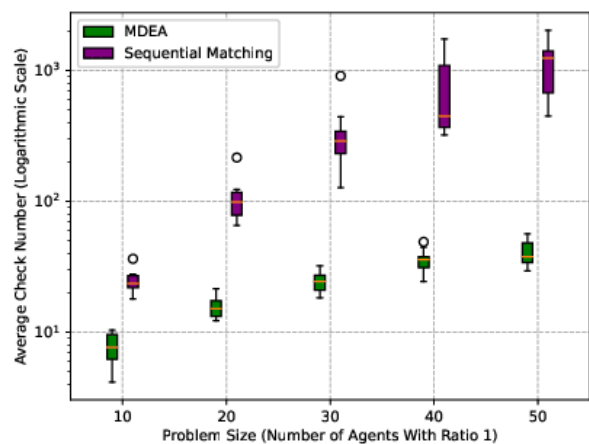
Fig. 5. Performance comparison between our MDEA algorithm and the analytical barrier approach in a 2D scenario. (a): Capture number comparison. (b): Check number comparison.

existing algorithms: the analytical barrier introduced in [18] for a 2D scenario and the sequential matching presented in [20] for a 3D scenario. To conduct our experiments, we use five groups of agents, maintaining a 1:1 ratio between defenders and attackers. The number of agents in each group ranges from 10 to 50, and we perform simulations with 10 different initial joint states for each group. We employ the same domain as described in Section V-A, with variations in the target sets for the different scenarios. Specifically, the 2D scenario has a rectangular domain of $[-5, 5]^2$ with the line segment $y = 5$ as the target set, while the 3D scenario has a box domain of $[-5, 5]^3$ with the flat face $z = -5$ as the target set.

During the simulation, we track two metrics to evaluate the effectiveness and computational efficiency of our proposed algorithm: the capture number, which represents the total number of attackers captured throughout the game, and the check number, denoting the number of convex programs of the form (17) computed within the multi-attack objective function



(a)



(b)

Fig. 6. Performance comparison between our MDEA algorithm and the sequential matching approach in a 3D scenario. (a): Capture number comparison. (b): Average check number comparison.

defined in (32). These metrics provide valuable insights into both the effectiveness and computational efficiency of our proposed algorithm. To ensure a fair comparison with other algorithms, we use a low capture radius of $r_i = 0.05(m)$ for the 2D scenario and $r_i = 0.2(m)$ for the 3D scenario. As in Section V-A, we adopt the attack strategy given in (27) and set the maximum speed ratios to 1.

We employ boxplots to display the results of our 2D simulation in Fig. 5, indicating that our MDEA algorithm outperforms the analytical barrier approach. Three colors are used to represent three cases: 1) MDEA applied at each allocation time; 2) analytical barrier, which performs allocation only at the initial joint state; 3) MDEA implemented solely at the initial joint state, akin to the analytical barrier. As illustrated in Fig. 5(a), MDEA yields a considerable improvement over the analytical barrier, with its median values consistently exceeding those of the analytical barrier. Furthermore, the capture number achieved by MDEA surpasses that attained

at the initial joint state, demonstrating the effectiveness of our approach as proven in Theorem 2. In Fig. 5(b), it can be observed that the analytical barrier exhibits a constant check number for each case, equal to the dimension of the decision variables in the ILP (34). Conversely, the check number of MDEA at the initial joint state is significantly lower than that of the analytical barrier, highlighting the superior computational efficiency of our method.

In the 3D simulation, our MDEA algorithm also outperforms the sequential matching method, as depicted in Fig. 6. We employ the same three colors to represent three cases as in the 2D simulation, with the analytical barrier replaced by sequential matching. As illustrated in Fig. 6(a), MDEA surpasses the sequential matching with higher median values of capture number. Moreover, MDEA attains a final capture number that exceeds the expected capture number initially obtained by the algorithm, thereby demonstrating the effectiveness of our approach in enhancing defense performance, as established in Theorem 2. Besides, Fig. 6(b) reveals that the average capture number achieved by MDEA is significantly lower than that of the sequential matching, where the average capture number is calculated by averaging the capture number of each step. This showcases the computational efficiency of our approach.

C. Gazebo Simulator with ROS

Finally, we take into account the collision avoidance among defenders, and with actual robot models. To consider the real-world scenario, we adopt the collision avoidance method proposed in [28] to avoid collisions between defenders. Our simulations, conducted using the Gazebo simulator and integrated within a ROS framework, evaluate our approach in both 2D and 3D convex environments. We compare two scenarios: one with attackers employing the optimal strategy (illustrated in Fig. 7(a), 7(b), 7(c), 8(a), 8(b), and 8(c)), and another with attackers utilizing the move-forward strategy (depicted in Fig. 7(d) and Fig. 8(d)). The simulation results reveal that our approach demonstrates superior performance when attackers adopt the move-forward strategy.

VI. CONCLUSION

In this paper, we introduced a comprehensive two-scale strategy for defender teams in multiplayer reach-avoid games, emphasizing real-time adaptability and scalability. Our proposed dual-mode switching algorithm for defense coordination effectively maximizes the defense-winning region while accommodating dynamic interactions between a coalition of defenders and a single attacker. Furthermore, we presented a monotonic defense enhancement algorithm for optimal defender allocation, utilizing a hierarchical iterative technique to manage multi-attack scenarios efficiently. As avenues for future research, the extension of our approach to non-convex environments and the incorporation of more complex agent models could further enhance the performance and applicability of our proposed framework in various real-world robotics applications.

APPENDIX

A. Proof of Proposition 1

Proof: To show the convexity of the SRS, we first exhibit that for each $i \in \mathcal{C}$, $c_{ij}(q, x_{ij})$ is convex with respect to q . Note that c_{ij} can be decomposed into a sum of three terms: $c_{ij}(q, x_{ij}) = (\gamma_{ij}^2 - 1)\|q\|^2 + 2r_i\gamma_{ij}\|q - p_j^a\| + [2(p_i^d - \gamma_{ij}^2 p_j^a)^T q + \gamma_{ij}^2\|p_j^a\|^2 - \|p_i^d\|^2 + r_i^2]$. Owing to the maximum speed ratio constraint (8) and the positivity of r_i , the coefficients of the first two terms are non-negative. Consequently, these two terms are convex, as the (squared) Euclidean norm is a convex function. The convexity of $c_{ij}(q, x_{ij})$ then follows from the fact that the last term is linear, and the sum of convex functions is itself a convex function.

It remains to establish that if $q \in \mathcal{D}$ satisfies the inequality $\max_{i \in \mathcal{C}} c_{ij}(q, x_{ij}) \leq 0$, then q belongs to the SRS. Given any such q , consider the constant attack strategy $\pi_j^a = v_{j,\max}^a \mathcal{N}(q - p_j^a)$ over the time interval $[0, \tau]$, where $\tau = \frac{\|q - p_j^a\|}{v_{j,\max}^a}$. The reachability property of the SRS holds by noting that attacker j can reach q from p_j^a along the line segment L connecting p_j^a and q using π_j^a . On the other hand, any point on L can be expressed as $q_\lambda = (1 - \lambda)p_j^a + \lambda q$ with parameter $\lambda \in [0, 1]$, which is reached by attacker j at time $\lambda\tau$ using π_j^a . Under the same time, the closest point to q_λ that defender i can reach from p_i^d , denoted by $q_{i,\lambda}^{d*}$, must lie on the straight line that connects p_i^d and q_λ , as defender i can move in any direction. This leads to $q_{i,\lambda}^{d*} = p_i^d + v_{i,\max}^d \frac{q_\lambda - p_i^d}{\|q_\lambda - p_i^d\|} \lambda\tau$. Besides, the convexity of $c_{ij}(q, x_{ij})$ implies that $c_{ij}(q_\lambda, x_{ij}) \leq (1 - \lambda)c_{ij}(p_j^a, x_{ij}) + \lambda c_{ij}(q, x_{ij}) \leq 0$, which in turn indicates that $s_i(q_{i,\lambda}^{d*}, q_\lambda) = r_i - \|\|q_\lambda - p_i^d\| - \gamma_{ij}\|q_\lambda - p_j^a\|\| = \gamma_{ij}\|q_\lambda - p_j^a\| + r_i - \|q_\lambda - p_i^d\| \leq 0$. As a result, for any admissible defense strategy π_i^d , $s_i(\chi_i^d(\lambda\tau; p_i^d, \pi_i^d), q_\lambda) \leq s_i(q_{i,\lambda}^{d*}, q_\lambda) \leq 0$ for all $\lambda \in [0, 1]$, yielding the safety property of the SRS. ■

B. Proofs of Proposition 2 and (24)

Proof: Consider the Lagrangian function of (17):

$$\begin{aligned} \mathcal{L}^d(\hat{q}, \hat{\lambda}) = & \|q - \hat{q}\|^2 + \sum_{i \in \mathcal{C}} \lambda_{ij} c_{ij}(q, x_{ij}) \\ & + \sum_{k \in \mathcal{I}_D} \bar{\lambda}_k d_k(q) + \sum_{l \in \mathcal{I}_G} \tilde{\lambda}_l g_l(\tilde{q}) \end{aligned}$$

where $\hat{q} = (q, \tilde{q})$ and $\hat{\lambda} = (\lambda_{ij}, i \in \mathcal{C}; \bar{\lambda}_k, k \in \mathcal{I}_D; \tilde{\lambda}_l, l \in \mathcal{I}_G)$ is the Lagrange multiplier. The KKT conditions asserts that for the optimal solution $\hat{q}^* = (\xi_j^C, \tilde{\xi}_j^C)$, there is a Lagrange multiplier $\hat{\lambda}^*$ with nonnegative components such that $\frac{\partial \mathcal{L}^d}{\partial \hat{q}}(\hat{q}^*, \hat{\lambda}^*) = 0$, i.e.,

$$2(\xi_j^C - \tilde{\xi}_j^C)^T + \sum_{i \in \mathcal{C}} \lambda_{ij}^* \frac{\partial c_{ij}}{\partial q}(\xi_j^C, x_{ij}) + \sum_{k \in \mathcal{I}_D} \bar{\lambda}_k^* \frac{\partial d_k}{\partial q}(\xi_j^C) = 0 \quad (43)$$

$$2(\xi_j^C - \tilde{\xi}_j^C)^T - \sum_{l \in \mathcal{I}_G} \tilde{\lambda}_l^* \frac{\partial g_l}{\partial \tilde{q}}(\tilde{\xi}_j^C) = 0. \quad (44)$$

Additionally, for any interior point $x_j^C \in \mathcal{D}'$ and any $i \in \mathcal{C}$, one of the following three cases occurs: i) $c_{ij}(\xi_j^C, x_{ij}) < 0$; ii)

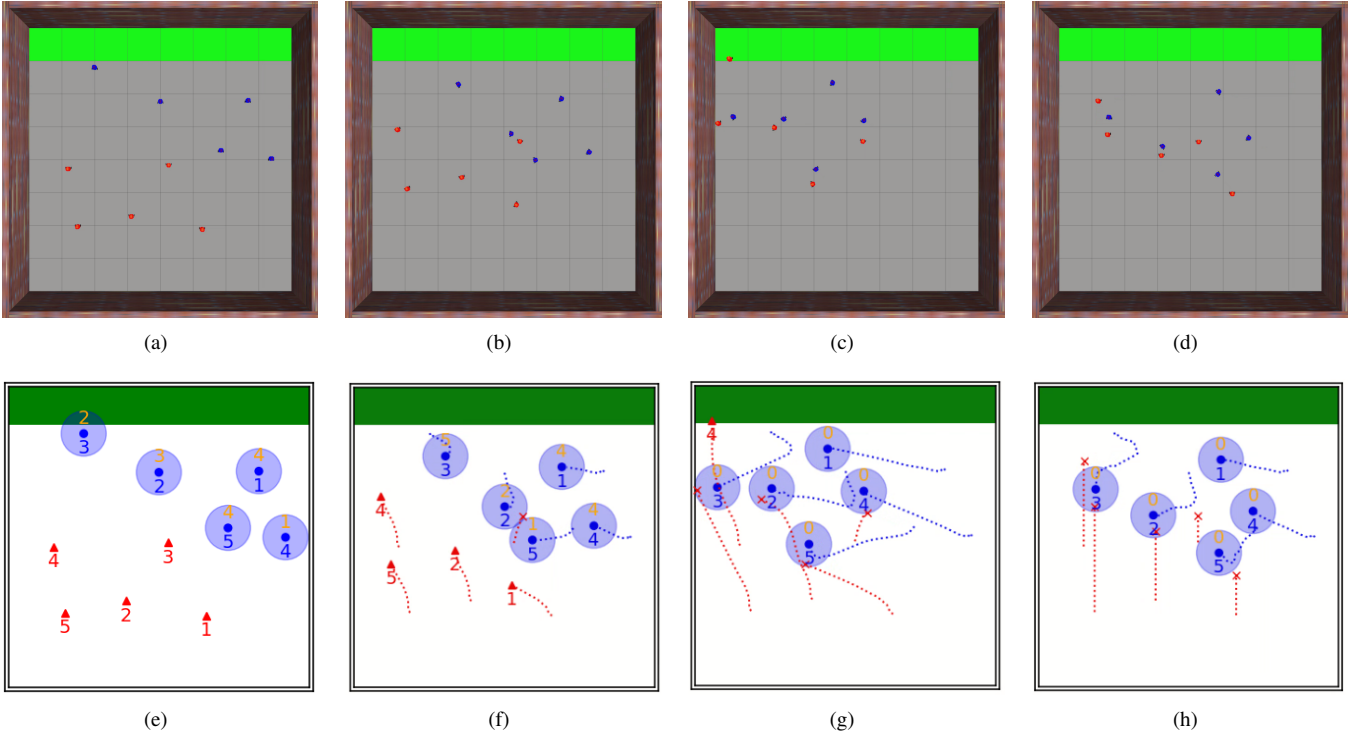


Fig. 7. A 2D simulation result for five defenders (blue circles) versus five attackers (red triangles).

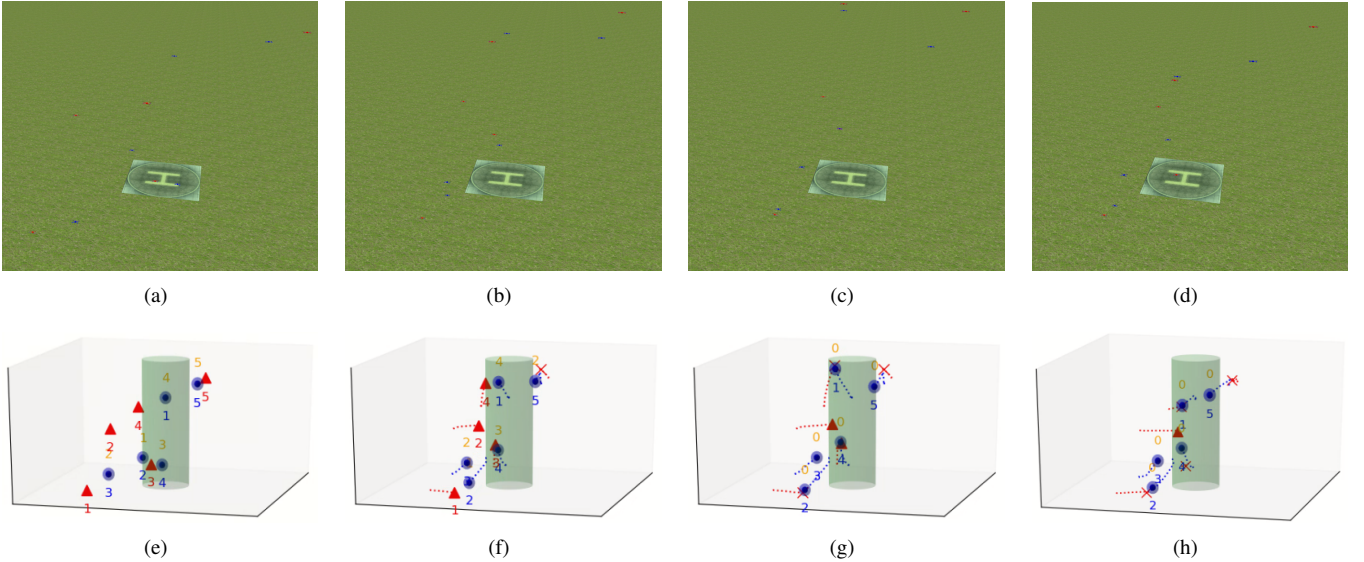


Fig. 8. A 3D simulation result for five defenders (blue spheres) versus five attackers (red triangles).

$c_{ij}(\xi_j^C, x_{ij}) = 0$ and $\dot{c}_{ij}(\xi_j^C, x_{ij}) = 0$; iii) $c_{ij}(\xi_j^C, x_{ij}) = 0$ and $\dot{c}_{ij}(\xi_j^C, x_{ij}) \neq 0$. In particular, since c_{ij} is continuously differentiable, the set of interior points for which the last case holds has measure zero, according to the results from real analysis [29]. Thus, the complementarity condition $\lambda_{ij}^* c_{ij}(\xi_j^C, x_{ij}) = 0$ implies that for almost every $x_j^C \in \mathcal{D}'$, $\lambda_{ij}^* \dot{c}_{ij}(\xi_j^C, x_{ij}) = 0$,

i.e.,

$$\lambda_{ij}^* \left(\frac{\partial c_{ij}}{\partial q}(\xi_j^C, x_{ij}) \dot{\xi}_j^C + \frac{\partial c_{ij}}{\partial p_i^d}(\xi_j^C, x_{ij}) u_i^d + \frac{\partial c_{ij}}{\partial p_j^a}(\xi_j^C, x_{ij}) u_j^a \right) = 0, \quad \forall i \in \mathcal{C}. \quad (45)$$

Similar derivations can be respectively employed to the complementarity conditions $\bar{\lambda}_k^* d_k(\xi_j^C) = 0$, $k \in \mathcal{I}_D$ and $\bar{\lambda}_l^* g_l(\tilde{\xi}_j^C) = 0$, $l \in \mathcal{I}_G$, yielding that for almost every $x_j^C \in \mathcal{D}'$,

$$\bar{\lambda}_k^* \frac{\partial d_k}{\partial q}(\xi_j^C) \dot{\xi}_j^C = 0, \quad \forall k \in \mathcal{I}_D \quad (46)$$

and $\tilde{\lambda}_l^* \frac{\partial g_l}{\partial q}(\tilde{\xi}_j^C) \dot{\xi}_j^C = 0$ for all $l \in \mathcal{I}_G$, where the latter equation together with (44) leads to

$$2(\xi_j^C - \tilde{\xi}_j^C)^T \dot{\xi}_j^C = \sum_{l \in \mathcal{I}_G} \tilde{\lambda}_l^* \frac{\partial g_l}{\partial q}(\tilde{\xi}_j^C) \dot{\xi}_j^C = 0. \quad (47)$$

Therefore,

$$\begin{aligned} \dot{\Phi}_j^C &\stackrel{\text{def}}{=} 2(\xi_j^C - \tilde{\xi}_j^C)^T (\dot{\xi}_j^C - \dot{\tilde{\xi}}_j^C) \\ &\stackrel{(47)}{=} 2(\xi_j^C - \tilde{\xi}_j^C)^T \dot{\xi}_j^C \\ &\stackrel{(43)}{=} - \sum_{i \in \mathcal{C}} \lambda_{ij}^* \frac{\partial c_{ij}}{\partial q}(\xi_j^C, x_{ij}) \dot{\xi}_j^C - \sum_{k \in \mathcal{I}_D} \tilde{\lambda}_k^* \frac{\partial d_k}{\partial q}(\xi_j^C) \dot{\xi}_j^C \\ &\stackrel{(45)+(46)}{=} \sum_{i \in \mathcal{C}} \lambda_{ij}^* \frac{\partial c_{ij}}{\partial p_i^d}(\xi_j^C, x_{ij}) u_i^d + \sum_{i \in \mathcal{C}} \lambda_{ij}^* \frac{\partial c_{ij}}{\partial p_j^a}(\xi_j^C, x_{ij}) u_j^a \end{aligned}$$

holds for almost every $x_j^C \in \mathcal{D}'$. This completes the proof of Proposition 2 by examining (18).

To verify the equality (24), we consider the Lagrangian function of (23):

$$\mathcal{L}^a(q, \hat{\mu}) = \|q - p_j^a\|^2 + \sum_{i \in \mathcal{C}} \mu_{ij} c_{ij}(q, x_{ij}) + \sum_{l \in \mathcal{I}_G} \tilde{\mu}_l g_l(q)$$

with the Lagrange multiplier $\hat{\mu} = (\mu_{ij}, i \in \mathcal{C}, \tilde{\mu}_l, l \in \mathcal{I}_G)$. Analogous to the proof of Proposition 2, the KKT conditions imply that there is a Lagrange multiplier $\hat{\mu}^*$ with nonnegative components such that

$$2(\bar{\xi}_j^C - p_j^a)^T + \sum_{i \in \mathcal{C}} \mu_{ij}^* \frac{\partial c_{ij}}{\partial q}(\bar{\xi}_j^C, x_{ij}) + \sum_{l \in \mathcal{I}_G} \tilde{\mu}_l^* \frac{\partial g_l}{\partial q}(\bar{\xi}_j^C) = 0 \quad (48)$$

and for almost every $x_j^C \notin \mathcal{D}_j^C$,

$$\begin{aligned} \mu_{ij}^* \left(\frac{\partial c_{ij}}{\partial q}(\bar{\xi}_j^C, x_{ij}) \dot{\xi}_j^C + \frac{\partial c_{ij}}{\partial p_i^d}(\bar{\xi}_j^C, x_{ij}) u_i^d \right. \\ \left. + \frac{\partial c_{ij}}{\partial p_j^a}(\bar{\xi}_j^C, x_{ij}) u_j^a \right) = 0, \quad \forall i \in \mathcal{C} \end{aligned} \quad (49)$$

and

$$\tilde{\mu}_l^* \frac{\partial g_l}{\partial q}(\bar{\xi}_j^C) \dot{\xi}_j^C = 0, \quad \forall l \in \mathcal{I}_G. \quad (50)$$

Consequently, the proof is done by noting that

$$\begin{aligned} \dot{\Phi}_j^C + 2(\bar{\xi}_j^C - p_j^a)^T u_j^a \\ \stackrel{\text{def}}{=} 2(\bar{\xi}_j^C - p_j^a)^T \dot{\xi}_j^C \\ \stackrel{(48)}{=} - \sum_{i \in \mathcal{C}} \mu_{ij}^* \frac{\partial c_{ij}}{\partial q}(\bar{\xi}_j^C, x_{ij}) \dot{\xi}_j^C - \sum_{l \in \mathcal{I}_G} \tilde{\mu}_l^* \frac{\partial g_l}{\partial q}(\bar{\xi}_j^C) \dot{\xi}_j^C \\ \stackrel{(49)+(50)}{=} \sum_{i \in \mathcal{C}} \mu_{ij}^* \frac{\partial c_{ij}}{\partial p_i^d}(\bar{\xi}_j^C, x_{ij}) u_i^d + \sum_{i \in \mathcal{C}} \mu_{ij}^* \frac{\partial c_{ij}}{\partial p_j^a}(\bar{\xi}_j^C, x_{ij}) u_j^a. \end{aligned} \quad \blacksquare$$

C. Proof of Proposition 3

Proof: The proof is conducted by contradiction. Suppose there are $q_1, q_2 \in \Omega_j^C(x_j^C)$ that result in $\Psi(q_1) = \Psi(q_2)$, where

$$\Psi(q) = \min_{\tilde{q} \in \mathcal{G}} \|q - \tilde{q}\|^2 \quad (51)$$

is the minimum squared distance from q to the target set. We claim that the line segment connecting q_1 and q_2 , denoted as $q_\lambda = \lambda q_1 + (1 - \lambda)q_2$ with parameter $\lambda \in [0, 1]$, must lie on the zero level set defined by $c_{kj}(q, x_{kj}) = 0$ for some $k \in \mathcal{N}$. First note that the line segment q_λ must lie within the SRS due to the convexity of the SRS. Next, the Definition of Φ_j^C yields that $\Phi_j^C(x_j^C) \leq \Psi(q)$ for all $q \in \Omega_j^C(x_j^C)$, and thus $\Phi_j^C(x_j^C) \leq \Psi(q_\lambda)$ for all $\lambda \in [0, 1]$. Additionally, since Ψ is convex, $\Psi(q_\lambda) \leq \lambda \Psi(q_1) + (1 - \lambda) \Psi(q_2) = \Phi_j^C(x_j^C)$. Therefore, $\Psi(q_\lambda) = \Phi_j^C(x_j^C)$ for all $\lambda \in [0, 1]$, implying that the line segment q_λ is on the boundary of the SRS. Finally, the claim is verified by noting that if $\max_{i \in \mathcal{N}} c_{ij}(q_{\lambda_0}, x_{ij}) < 0$ for some $\lambda_0 \in [0, 1]$, then the point q_{λ_0} lies strictly within the SRS, which would contradict the result that q_{λ_0} lies on the boundary of the SRS. However, the claim violates the fact that the zero level set defined by $c_{kj}(q, x_{kj}) = 0$ contains no line segments. This is because $(q_1 - q_2)^T \nabla_q c_{kj} = 0$ can never have infinite solutions, where $\nabla_q c_{kj} = 2(\gamma_{kj}^2 - 1)q + 2r_k \gamma_{kj} \frac{q - p_j^a}{\|q - p_j^a\|} + 2(p_k^d - \gamma_{kj}^2 p_j^a)$ is the normal vector to the zero level set of $c_{kj}(q, x_{kj}) = 0$. \blacksquare

D. Proof of Proposition 4

Proof: It suffices to show by contradiction that $\Phi_j^{C'}(x_j^{C'}) = \Phi_j^C(x_j^C)$ with $C' = \Lambda_j^C$, or equivalently $\Psi(\xi_j^{C'}) = \Psi(\xi_j^C)$ in which Ψ is defined in (51). Assuming that $\Psi(\xi_j^{C'}) \neq \Psi(\xi_j^C)$. Then $\Psi(\xi_j^{C'}) < \Psi(\xi_j^C)$ as $\xi_j^{C'} \in \Omega_j^{C'}$. To reach a contradiction, we consider the line segment connecting $\xi_j^{C'}$ and ξ_j^C parameterized by $\mu \in [0, 1]$ given as $\xi_\mu = \mu \xi_j^{C'} + (1 - \mu) \xi_j^C$. Since C' is the ADS for (\mathcal{C}, j) , it follows that $c_{ij}(\xi_j^{C'}, x_{ij}) < 0$ for all $i \in \mathcal{C} \setminus C'$. By the continuity of $c_{ij}(\xi_\mu, x_{ij})$ with respect to μ , there exists $\mu_i \in (0, 1)$ for each $i \in \mathcal{C} \setminus C'$ such that $c_{ij}(\xi_\mu, x_{ij}) \leq 0$ for all $\mu \in [0, \mu_i]$. Let $\bar{\mu}$ be the minimum of all μ_i . Then $c_{ij}(\xi_{\bar{\mu}}, x_{ij}) \leq 0, \forall i \in \mathcal{C} \setminus C'$. Additionally, since the line segment ξ_μ lies within $\Omega_j^{C'}(x_j^{C'})$, it yields that $c_{ij}(\xi_{\bar{\mu}}, x_{ij}) \leq 0, \forall i \in C'$. As a result, $\xi_{\bar{\mu}} \in \Omega_j^C$. However, $\Psi(\xi_{\bar{\mu}}) \leq \bar{\mu} \Psi(\xi_j^{C'}) + (1 - \bar{\mu}) \Psi(\xi_j^C) < \Psi(\xi_j^C)$, which contradicts the fact that the minimum value of Ψ occurs at ξ_j^C . \blacksquare

E. Proof of Proposition 5

Proof: According to Proposition 4, it is sufficient to establish that for any feasible coalition-attacker pair (\mathcal{C}, j) with $|\Lambda_j^C| > n$, there exists a subset C' of Λ_j^C with $|C'| \leq n$ such that $\Phi_j^{C'}(x_j^{C'}) = \Phi_j^C(x_j^C)$. For each $i \in \Lambda_j^C$, the almost-optimal waypoint ξ_j^C lies on the tangent of the zero level set $c_{ij}(\xi_j^C, x_{ij}) = 0$, and thus satisfies the linear equation $(q - \xi_j^C)^T \nabla_q c_{ij}(\xi_j^C, x_{ij}) = 0$, where $\nabla_q c_{ij}(\xi_j^C, x_{ij})$ is the normal vector of $c_{ij}(q, x_{ij}) = 0$ at $q = \xi_j^C$. Since an n -dimensional solution can be uniquely determined by at most n independent linear equations, there is a subset C' of Λ_j^C with $|C'| \leq n$ such that ξ_j^C is the unique solution to the linear equations $(q - \xi_j^C)^T \nabla_q c_{ij}(\xi_j^C, x_{ij}) = 0$ for all $i \in C'$. Moreover, due to the sublevel set representation of Ω_j^C , C' can be chosen in a way that $U \cap \Omega_j^C = U \cap \Omega_j^{C'}$ for some neighborhood U of ξ_j^C . Consequently, by the convexity of the SRS, we can conclude that $\Phi_j^{C'}(x_j^{C'}) = \Phi_j^C(x_j^C)$. \blacksquare

F. Proof of Proposition 6

Proof: Optimality: Note that the maximum possible value that the multi-attack objective function Γ could attain is equal to the number of active attackers j for which the coalition-attacker pair (\mathcal{N}, j) is feasible. In view of Algorithm 3, an index j is removed from \mathcal{M}_r after the first iteration if and only if (\mathcal{N}, j) is infeasible or attacker j is included in the suboptimal solution $\tilde{\Theta}_1$. Hence, the emptiness of \mathcal{M}_r after the first iteration indicates that $\tilde{\Theta}$ achieves the maximum possible value of Γ , making it an optimal solution to the ILP (34).

Efficiency: In each iteration of Algorithm 3, there are two steps that require the computation of the convex program of the form (17): to determine the feasibility of the coalition-attacker pair (\mathcal{N}_r, j) , and to find all irreducible sub-pairs of $(\Lambda_j^{\mathcal{N}_r}, j)$. The former step requires only one calculation, while the latter step performed using Algorithm 2, requires at most $\sum_{k=1}^{n-1} \binom{n}{k} = 2^n - 2$ computations given that the cardinality of the ADS is no more than n . Hence, the total number of computations at this iteration for one attacker is at most $2^n - 1$. Additionally, the number of iterations is limited by the number of active attackers M_a , as at least one attacker is removed from the set \mathcal{M}_r after each iteration. The total number of calculations for all iterations is therefore at most $\sum_{k=1}^{M_a} (2^n - 1)k$, which is less than $2^{n-1}M_a(1 + M_a)$. ■

REFERENCES

- [1] R. Vidal, O. Shakernia, H. J. Kim, D. H. Shim, and S. Sastry, "Probabilistic pursuit-evasion games: theory, implementation, and experimental evaluation," *IEEE transactions on robotics and automation*, vol. 18, no. 5, pp. 662–669, 2002.
- [2] S. Bansal, M. Chen, S. Herbert, and C. J. Tomlin, "Hamilton-jacobi reachability: A brief overview and recent advances," in *2017 IEEE 56th Annual Conference on Decision and Control (CDC)*, 2017, pp. 2242–2253.
- [3] C. Robin and S. Lacroix, "Multi-robot target detection and tracking: taxonomy and survey," *Autonomous Robots*, vol. 40, pp. 729–760, 2016.
- [4] E. Bakolas and P. Tsiotras, "Relay pursuit of a maneuvering target using dynamic voronoi diagrams," *Automatica*, vol. 48, no. 9, pp. 2213–2220, 2012.
- [5] A. Pierson, Z. Wang, and M. Schwager, "Intercepting rogue robots: An algorithm for capturing multiple evaders with multiple pursuers," *IEEE Robotics and Automation Letters*, vol. 2, no. 2, pp. 530–537, 2016.
- [6] H. Huang, J. Ding, W. Zhang, and C. J. Tomlin, "A differential game approach to planning in adversarial scenarios: A case study on capture-the-flag," in *2011 IEEE International Conference on Robotics and Automation*. IEEE, 2011, pp. 1451–1456.
- [7] M. Jaderberg, W. M. Czarnecki, I. Dunning, L. Marris, G. Lever, A. G. Castaneda, C. Beattie, N. C. Rabinowitz, A. S. Morcos, A. Ruderman *et al.*, "Human-level performance in 3d multiplayer games with population-based reinforcement learning," *Science*, vol. 364, no. 6443, pp. 859–865, 2019.
- [8] D. Shishika, J. Paulos, and V. Kumar, "Cooperative team strategies for multi-player perimeter-defense games," *IEEE Robotics and Automation Letters*, vol. 5, no. 2, pp. 2738–2745, 2020.
- [9] S. Velhal, S. Sundaram, and N. Sundararajan, "A decentralized multi-robot spatiotemporal multitask assignment approach for perimeter defense," *IEEE Transactions on Robotics*, 2022.
- [10] K. Margellos and J. Lygeros, "Hamilton-jacobi formulation for reach-avoid differential games," *IEEE Transactions on automatic control*, vol. 56, no. 8, pp. 1849–1861, 2011.
- [11] M. Chen, Z. Zhou, and C. J. Tomlin, "Multiplayer reach-avoid games via pairwise outcomes," *IEEE Transactions on Automatic Control*, vol. 62, no. 3, pp. 1451–1457, 2016.
- [12] T. Başar and G. J. Olsder, *Dynamic noncooperative game theory*. SIAM, 1998.
- [13] Z. Zhou, J. Ding, H. Huang, R. Takei, and C. Tomlin, "Efficient path planning algorithms in reach-avoid problems," *Automatica*, vol. 89, pp. 28–36, 2018.
- [14] R. Isaacs, *Differential games: a mathematical theory with applications to warfare and pursuit, control and optimization*. Courier Corporation, 1999.
- [15] E. Garcia, D. W. Casbeer, and M. Pachter, "Optimal strategies for a class of multi-player reach-avoid differential games in 3d space," *IEEE Robotics and Automation Letters*, vol. 5, no. 3, pp. 4257–4264, 2020.
- [16] E. Garcia, D. W. Casbeer, A. Von Moll, and M. Pachter, "Multiple pursuer multiple evader differential games," *IEEE Transactions on Automatic Control*, vol. 66, no. 5, pp. 2345–2350, 2020.
- [17] R. Yan, Z. Shi, and Y. Zhong, "Reach-avoid games with two defenders and one attacker: An analytical approach," *IEEE transactions on cybernetics*, vol. 49, no. 3, pp. 1035–1046, 2018.
- [18] —, "Task assignment for multiplayer reach-avoid games in convex domains via analytical barriers," *IEEE Transactions on Robotics*, vol. 36, no. 1, pp. 107–124, 2019.
- [19] Z. Zhou, W. Zhang, J. Ding, H. Huang, D. M. Stipanović, and C. J. Tomlin, "Cooperative pursuit with voronoi partitions," *Automatica*, vol. 72, pp. 64–72, 2016.
- [20] R. Yan, X. Duan, Z. Shi, Y. Zhong, and F. Bullo, "Matching-based capture strategies for 3d heterogeneous multiplayer reach-avoid differential games," *Automatica*, vol. 140, p. 110207, 2022.
- [21] Z. Deng and Z. Kong, "Multi-agent cooperative pursuit-defense strategy against one single attacker," *IEEE Robotics and Automation Letters*, vol. 5, no. 4, pp. 5772–5778, 2020.
- [22] I. M. Mitchell *et al.*, "A toolbox of level set methods," *UBC Department of Computer Science Technical Report TR-2007-11*, p. 31, 2007.
- [23] F. Blanchini, "Set invariance in control," *Automatica*, vol. 35, no. 11, pp. 1747–1767, 1999.
- [24] J. Nocedal and S. Wright, *Numerical optimization*. Springer Science & Business Media, 2006.
- [25] B. P. Gerkey and M. J. Mataric, "A formal analysis and taxonomy of task allocation in multi-robot systems," *The International journal of robotics research*, vol. 23, no. 9, pp. 939–954, 2004.
- [26] S. Diamond and S. Boyd, "Cvxpy: A python-embedded modeling language for convex optimization," *The Journal of Machine Learning Research*, vol. 17, no. 1, pp. 2909–2913, 2016.
- [27] N. Koenig and A. Howard, "Design and use paradigms for gazebo, an open-source multi-robot simulator," in *2004 IEEE/RSJ International Conference on Intelligent Robots and Systems (IROS)(IEEE Cat. No. 04CH37566)*, vol. 3. IEEE, 2004, pp. 2149–2154.
- [28] L. Wang, A. D. Ames, and M. Egerstedt, "Safety barrier certificates for collisions-free multirobot systems," *IEEE Transactions on Robotics*, vol. 33, no. 3, pp. 661–674, 2017.
- [29] H. L. Royden and P. Fitzpatrick, *Real analysis*. Macmillan New York, 1988, vol. 32.